# $Ca^{2+}$-dependent $K^+$ currents and spike-frequency adaptation in medial entorhinal cortex layer II stellate cells

Farhan A Khawaja
Department of Neurology and Neurosurgery
McGill University, Montreal
August, 2006

A thesis submitted to McGill University in partial fulfillment of
the requirements of the degree of
Master of Science

*Your file Votre référence*
*ISBN: 978-0-494-32730-2*
*Our file Notre référence*
*ISBN: 978-0-494-32730-2*

*To Al-Hadi*

# Table of Contents

# Abstract

We hypothesized that stellate cells (SCs) from layer II of the medial entorhinal cortex (MEC) may express currents that underlie spike-frequency adaptation (SFA) and that inhibitory modulation of these currents may permit the non-adapting nature of pulse-evoked post-burst after-discharges, a possible neuronal correlate of the post-stimulus delay firing seen *in-vivo* during working memory (WM) tasks. It was revealed that SCs contain medium ($mI_{K(Ca)}$) and slow ($sI_{AHP}$) $Ca^{2+}$-dependent $K^+$ currents. Furthermore, it was determined that $mI_{K(Ca)}$ is not mediated by apamin-sensitive SK channels in SCs, whereas it was found to be is apamin-sensitive in MEC layer II non-SCs. In addition, the results indicated that $mI_{K(Ca)}$ and $sI_{AHP}$ may underlie SFA in SCs and that $mI_{K(Ca)}$, $sI_{AHP}$ and SFA are subject to inhibitory modulation by PKA-activation. Therefore, PKA modulation may be important for SCs to exhibit post-burst after-discharges. Future work is required to determine whether PKA modulation of MEC layer II SCs plays an important role during WM tasks.

# Résumé

Nous émettions l'hypothèse que les cellules stellaires (CS) issues de la couche II du cortex enthorinal médian (CEM) peuvent générer des courants qui sous-tendent le phénomène d'adaptation de la fréquence de décharge (AFD). L'inhibition de ces courants permettrait la nature non adaptative du post-burst après-décharge, une possible corrélation neuronale du délai de décharge post-stimulus observée *in vivo* durant les tâches de mémoire de travail (MT). Il a été démontré que les CS contiennent les courants $K^+$ dépendant du $Ca^{2+}$ de type moyen ($mI_{K(Ca)}$) et de type lent ($sI_{AHP}$). De plus, il a été déterminé que les courants $mI_{K(Ca)}$ ne sont pas médiés par les canaux SK sensibles à l'apamine dans les CS alors qu'ils le sont dans les cellules non stellaires de la couche II du CEM. D'autres résultats ont montré que les courants $mI_{K(Ca)}$ et $sI_{AHP}$ pourraient être la cause du phénomène de AFD dans les CS et qu'ils pourraient être sujet à une modulation inhibitrice via l'activation de la protéine kinase de type A (PKA). En effet, la modulation de la PKA par des neurotransmetteurs in vivo pourrait être importante pour les CS afin d'exprimer les post-burst après-décharges. Plus d'investigations de ce processus de modulation via PKA dans les CS de la couche II du CEM et de son rôle *in vivo* dans les tâches de MT se révèlent nécessaires.

# Acknowledgments

First and foremost, I extend my heart-felt thanks to my family: my parents Dr. Abdur Rahman and Farah Khawaja and my brother Irfan. Their love and guidance has enabled me to excel in my education. I love them very much.

The late Dr. Angel Alonso was my previous thesis supervisor. His magnificent supervision allowed me to easily adapt into an experimental setting from my prior theoretical background. He was a great teacher, supervisor and friend. His passion for science provided me with the inspiration to learn and grow as a student. I will always miss him.

My deepest gratitude is extended towards Dr. Charles W. Bourque, my current co-supervisor. His guidance has allowed me to strive towards my potential as a scientist. In particular, through his training, I have become more independent, intelligent and patient. Moreover, his training has enabled the enhancement of my analytical and communication abilities. The completion of this thesis would not have been possible without his support.

I also thank my co-supervisor Dr. David S. Ragsdale for the vital support he has given in administrative and scientific matters.

In addition, I express thanks to my colleagues in *Alonso Lab*: Babak Tahvildari and Drs. Motoharu Yoshida and Antonio Reboreda. They were the heart of an enriching lab environment, conducive to scientific research. The time we shared is priceless.

I thank Dr. Ruby Klink, a previous member of *Alonso Lab*, for teaching me the whole-cell patch clamp technique using an *in-vitro* slice preparation. She has been a great friend and mentor, providing our lab the support it needed during times of difficulty.

There are numerous scientists who assisted me in various ways throughout my research training. These include Drs. Barbara Jones, Clayton Dickson, Michael Hasselmo, Wendy Suzuki, Howard Eichenbaum, Mortimer Mishkin, Erik Fransen and Bob Foehring. Their support is greatly appreciated.

I thank Monique Ledermann and Naomi Takeda for their assistance during my graduate studies at the Montreal Neurological Institute. They were never too busy to answer my questions.

Moreover, I am grateful toward Oum Hassani and Frèdèric Brischoux for the French translation of the thesis abstract.

Finally, I thank the Montreal Neurological Institute, the Faculty of Medicine and CIHR for providing the funding for my graduate studies.

# Associated Publications

## Refereed Abstracts

F.A. Khawaja, A. Alonso. THE SLOW AFTERHYPERPOLARIZATION OF ENTORHINAL CORTEX LAYER II STELLATE CELLS Program No. 736.7. *2005 Abstract Viewer/Itinerary Planner.* Washington, DC: Society for Neuroscience, 2005. Online.

Control of Spike Frequency Adaptation in Medial Entorhinal Cortex Layer II Stellate Cells Khawaja, Farhan A.; Alonso, Angel; Bourque, Charles W. *J Physiol* (2006) **J Physiol C103**

## Paper

$Ca^{2+}$-dependent $K^{+}$ currents and spike-frequency adaptation in medial entorhinal cortex layer II stellate cells. Khawaja, Farhan A.; Alonso, Angel; Bourque, Charles W., 2007 (submitted).

# List of Abbreviations

| | |
|---|---|
| ACSF | artificial cerebrospinal fluid |
| AHP | afterhyperpolarization |
| BK channel | big-conductance voltage-dependent $Ca^{2+}$-dependent $K^+$ channel |
| cAMP | 3'-5'-cyclic adenosine mono-phosphate |
| DMS | delayed matching-to-sample |
| DNMS | delayed non-matching-to-sample |
| EC | entorhinal cortex |
| $E_{Cl}$ | Nernst potential for chloride |
| $E_K$ | Nernst potential for potassium |
| $E_{Na}$ | Nernst potential for sodium |
| $Gluc^-$ | gluconate anion |
| HS | hyperpolarization-induced depolarizing sag |
| $I_{AHP}$ | afterhyperpolarization current |
| $I_C$ | voltage-dependent $Ca^{2+}$-dependent $K^+$ current |
| $I_h$ | h-current |
| $I_M$ | M-current |
| KGluc | potassium gluconate |
| $KMeSO_4$ | potassium methylsulfate |
| LEA | lateral entorhinal are |
| LEC | lateral entorhinal cortex |
| mAHP | medium afterhyperpolarization |
| MEC | medial entorhinal cortex |
| $MeSO_4^-$ | methylsulfate anion |
| $mI_{AHP}$ | medium AHP current |
| $mI_{K(Ca)}$ | medium $Ca^{2+}$-dependent $K^+$ AHP current |
| MTL | medial temporal lobe |
| NCM | non-specific cationic muscarinic |
| non-SC | non-stellate cells |
| PKA | protein kinase A |
| POR | postrhinal cortex |
| PR | perirhinal cortex |
| RMP | resting membrane potential |
| RP | rebound potential |
| sAHP | slow afterhyperpolarization |

| | |
|---|---|
| SCs | stellate cells |
| SFA | spike-frequency adaptation |
| $sI_{AHP}$ | slow $Ca^{2+}$-dependent $K^+$ AHP current |
| SK channel | small-conductance apamin-sensitive $Ca^{2+}$-dependent $K^+$ channel |
| WM | working memory |

# CHAPTER 1: Introduction

## 1.1) Overview

Working memory (WM) (or short-term memory) is a type of memory that is temporarily active (i.e. scale of seconds or minutes) and has a limited capacity (Goldman-Rakic, 1995). It is believed that information to be encoded in WM is first processed successively by sensory (Pasternak and Greenlee, 2005) and associational cortices (Goldman-Rakic, 1995), followed by areas of the medial temporal lobe (MTL) (Olson et al., 2006a; Olson et al., 2006b). This information may then flow backward through reciprocal connections to enable WM retrieval (Goldman-Rakic, 1995; Tomita et al., 1999; Olson et al., 2006b). Despite numerous studies that have been conducted to understand the mechanisms underlying WM (Baddeley, 2003; Pasternak and Greenlee, 2005), most of its aspects remain unknown. Nevertheless, a cellular mechanism that may be essential for this process is the ability of a subset of neurons from the entorhinal cortex (EC) called "stellate cells" (SCs) to generate post-burst firing activity during the period that corresponds to the time interval during which relevant information must be "held" in WM (Magistretti et al., 2004; Fransen, 2005). An unusual aspect of these neurons is their ability to display post-burst firing activity in a "non-adapting" manner. This indicates that SCs either do not express currents that mediate adaptation or that these currents are expressed, but inhibited when these neurons exhibit sustained activity. Even though it appears that SCs might express currents that mediate adaptation (Alonso and Klink, 1993), experiments have not validated the existence of these currents. As a result, the first aim of this thesis is to establish if there are currents that may contribute to adaptation

in SCs. It has been proposed that modulation by neurotransmitters may inhibit adaptation and enable non-adapting sustained activity in SCs (Klink and Alonso, 1997a; Magistretti et al., 2004; Fransen, 2005). It has been shown in other neurons that this modulation may be dependent on the enzyme "protein kinase A" (Pedarzani and Storm, 1993). Therefore, this thesis will examine if currents underlying adaptation can be modulated in SCs. In order to clarify the details of the basis for the hypotheses that were tested by the experimental work presented, relevant background literature will first be reviewed.

## 1.2) The EC

### *1.2.1) Location of the EC*

The EC is located in the MTL of the brain (Squire et al., 2004). Figure 1.1 highlights several areas of the MTL, including the medial entorhinal area/cortex (MEA or MEC), lateral entorhinal area/cortex (LEA or LEC), the perirhinal cortex (PR; areas 35 and 36) and the postrhinal cortex (POR) (Burwell and Amaral, 1998a). Today, it is generally believed that the MTL is an important area of the brain for memory, an idea which was first proposed by Scoville and Milner (Scoville and Milner, 1957).

### *1.2.2) Functional role of the MTL (lesion studies in humans) in memory formation*

The functional role of the MTL was first revealed by a human lesion study conducted by Scoville and Milner, (1957). In one of the cases of this study, a human male patient known as H.M. underwent bilateral removal of most of the components of his MTLs, including the hippocampal regions, most of the amygdaloid complexes and most of the PRs and ECs (Scoville and Milner, 1957; Corkin et al., 1997). The surgery

was undertaken because H.M. suffered from generalized seizures which were not adequately alleviated by heavy anticonvulsant drug treatment and whose frequency and severity continued to increase (Scoville and Milner, 1957). Following surgery, H.M.'s seizures were alleviated, but he was unable to remember everyday events which occurred after the operation (Scoville and Milner, 1957; Kandel, 2000). This was surprising because the operation was expected to only alleviate convulsions; however, it resulted in a memory defect as well. H.M. could still recollect events which had occurred prior to 19 months before the surgery (Scoville and Milner, 1957). Also, he scored as well as control subjects on tests that measured his intellectual and perceptual abilities (Scoville and Milner, 1957). Subsequent human lesion studies have also suggested that patients develop forgetfulness of everyday events after bilateral MTL lesions (as reviewed in Squire et al., 2004), whereas perceptual and intellectual abilities of these patients are usually not affected (Schmolck et al., 2000; Schmolck et al., 2002; Squire et al., 2004). These studies have indicated that the MTL is essential for the formation of new memories, a process known as memory consolidation, but is not required for memories that have already been stored.

### *1.2.3) Functional role of the MTL (lesion studies in humans) in WM*

Recent studies have examined patients with MTL lesions to determine if the MTL is an essential area of the brain for WM processing (Baddeley and Warrington, 1970; Cave and Squire, 1992; Olson et al., 2006a; Olson et al., 2006b). For example, in a study done by Olson et al. (2006a), control patients and those with bilateral MTL lesions (caused by brain pathology rather than by surgery) were required to recall either spatial locations or faces after a delay period of 4 seconds. Compared to control, WM was

significantly impaired in patients with bilateral MTL lesions in both of these experiments. In another study by Olson et al., 2006b, control patients and those with bilateral MTL damage (also caused by brain pathology) were required to remember object-location pairs for 8 seconds. Yet again, the performance of MTL lesioned patients was significantly lower than control. These studies suggested that the MTL as a whole may be critical for WM processing (Olson et al., 2006a; Olson et al., 2006b); however, it was still unclear how specific areas of the MTL may be involved. Before discussing how a specific region of the MTL (i.e. the EC) may be involved in WM, it is important to describe MTL circuitry.

### *1.2.4) MTL circuitry*

The interconnections of the MTL were first revealed in the monkey (Insausti et al., 1987a, b; Suzuki and Amaral, 1994) and later in the rat (Burwell et al., 1995; Insausti et al., 1997). The EC receives input from unimodal and polymodal association areas of the frontal, temporal and parietal lobes via the PR and POR (see Figure 1.2) (Squire et al., 2004). Next, the EC sends input to the hippocampal region, which contains the dentate gyrus, CA3, CA1 and the subiculum (Squire et al., 2004), which comprise successive elements of the forward pathway of the circuit (Figure 1.2). The output from the hippocampal region projects back to entorhinal neurons, which in turn innervate the PR and POR. This "backward" circuitry is completed with reciprocal projections from the POR and PR to the same cortical unimodal and polymodal association areas, from which the forward projections originated (Figure 1.2). Note that the EC resides in the middle of the circuit and therefore appears to serve as a "gateway" between higher cortical areas and the hippocampal region (Alonso and Klink, 1993; Klink and Alonso, 1997a). This

observation is consistent with its role as an important component of the MTL memory system. Furthermore, SCs located in the superficial layers of the EC serve as one of the most prominent target cell types within the EC for inputs arising from higher cortical areas, and these same cells provide most of the output from the EC to the hippocampal region (Insausti et al., 1997; Klink and Alonso, 1997b). This suggests that most of the information arriving from higher cortical areas may be processed by SCs before reaching the hippocampal region (Alonso and Llinas, 1989; Alonso and Klink, 1993). As explained earlier (see section 1.2.3), the MTL as a whole may be an important area of the brain for WM. Since the EC is centrally located in the MTL memory circuit, it may play an important role during WM processing. Indeed, animal lesion studies (Meunier et al., 1993; Leonard et al., 1995) have indicated that the EC may play an important functional role in WM.

### *1.2.5) Functional role of the EC (lesion studies in animals) in WM*

Studies with nonhuman primates have investigated the specific role of the EC in WM (Meunier et al., 1993; Leonard et al., 1995). The delayed matching-to-sample (DMS) task or the delayed non-matching-to-sample (DNMS) task are common paradigms used in these studies to measure WM performance (Meunier et al., 1993; Leonard et al., 1995). In these tasks, a sample visual stimulus is initially presented. Then, the subject is trained to hold (i.e. remember) the stimulus in WM during a "delay period." After the delay period, a test stimulus is presented (recognition phase). The subject must respond by indicating if the test stimulus matches (i.e. the DMS task) or does not match (i.e. the DNMS task) the sample stimulus. During such experiments, success is measured by the mean percentage of correct responses observed during a series of trials. These tests are

simple to use and are good indicators of WM performance because subjects must remember a stimulus for a short period of time (i.e. scale of seconds or minutes) and be able to distinguish it from novel stimuli. Using a DNMS protocol with visual stimuli, Meunier et al. (1993) tested control and lesioned monkeys with a delay period of 10 s, 30 s, 60 s and 120 s. In particular, they tested WM performance after combined and separate lesions of the PR and EC. Statistical analyses of these studies determined that lesions of the PR alone result in memory impairment comparable to combined lesions of the PR and EC, whereas lesions of the EC alone produced a mild, but significant deficit. In another study, Leonard et al. (1995) observed that monkeys with EC lesions show a significant impairment in task performance when the delay period is either 10 min or 40 min, but not when the delay periods are 8 s, 15 s or 30 s. These differences between control and EC lesioned monkeys indicated that the EC may be responsible for holding stimuli in memory for long delay periods during these tasks (Leonard et al., 1995). Subsequent studies assessed EC's functional role by recording *in-vivo* from single units during WM tasks (Suzuki et al., 1997; Young et al., 1997).

### *1.2.6) Functional role of the EC (in-vivo electrophysiological studies) in WM*

In-vivo electrophysiological studies have recorded from entorhinal neurons while animals perform WM tasks (Suzuki et al., 1997; Young et al., 1997). For example, Suzuki et al. (1997) reported that EC neurons may show changes in electrical activity when objects and places are used as visual stimuli in a DMS task (see section 1.2.5 for definition). In this study, all EC neurons that were analyzed showed a response (i.e. a change in action potential firing rate) in at least one of the stages of the task. In particular, a relatively large number of EC neurons showed significantly greater firing

frequency during the delay period (1 second) of the task, compared to other stages (Suzuki et al., 1997). This post-stimulus activity was sustained (i.e. did not show any adaptation) and was greater than the baseline frequency observed before stimulus presentation. The authors proposed that this post-stimulus delay firing may be a way by which EC neurons encode and retain information about the sample stimulus in WM during the delay period; however, the mechanism by which the stimulus would then be recognized during the subsequent recognition phase is unknown (Suzuki et al., 1997).

In a similar study, Young et al. (1997) recorded the electrical activity of cells from various areas of the MTL, including superficial layers of the EC, the PR and the subiculum (see Figure 1.2 for MTL circuit diagram). Firing rate was measured while the rat performed a DNMS task (see section 1.2.5 for definition), in which it was required to smell an odor, hold it in WM for a specific period of time (either 3 or 30 seconds) and then distinguish between the initial odor and other odors (Young et al., 1997). As in the previous study (Suzuki et al., 1997), almost all cells recorded from the EC displayed activity that was related to at least one of the stages of the task (Young et al., 1997). In addition, changes in the activity of cells from the subiculum and PR were also related to at least one of the stages of the task. However, compared to cells from the PR (~3%) and subiculum (~1%), a significantly larger proportion of EC cells from superficial layers (~15%) showed post-stimulus firing activity during the delay period (Young et al., 1997). As mentioned before, this delay period corresponds to the time during which the stimulus must be held in WM (see above in this section). Therefore, the studies by Young et al., 1997 and Suzuki et al., 1997 suggested that neurons from superficial layers of the EC may have a specialized function in the MTL of holding stimuli in WM during the delay period. Although the subtypes of EC neurons showing post-stimulus delay firing were

not identified in these studies, previous work has shown that SCs located in the superficial layers of the EC represent the major type of neuron interconnected to the PR, POR and the hippocampal region (see Figure 1.2). It is therefore reasonable to hypothesize that some of the neurons that display delay firing during WM include SCs.

## 1.3) A possible neuronal correlate of WM

### *1.3.1) Advantages of the whole-cell patch clamp technique*

Superficial layers I, II and III of the EC receive input from the PR and POR (see Figure 1.2 for MTL circuitry) and MEC layer II SCs serve as one of the major recipients of this input (Insausti et al., 1997; Burwell and Amaral, 1998b). EC neurons were recorded *in-vivo* in the electrophysiological experiments discussed in the last section (see section 1.2.6). In contrast to the difficulties involved in cell identification during these *in-vivo* studies involving behavioral experiments (section 1.2.6), both the specific type of neuron and the layer it occupies within the EC can be identified easily during whole-cell patch clamp recordings in *in-vitro* slice preparations (see section 2.3 for detailed explanation).

### *1.3.2) Voltage response of MEC layer II SCs to a brief depolarizing current pulse*

The whole-cell patch clamp technique was employed to record from MEC layer II SCs. Voltage responses were evoked in SCs (Figure 1.3A - Khawaja and Alonso, 2005 unpublished data) by applying 50 pA depolarizing current pulses lasting 1 s (shown below the voltage trace in Figure 1.3A) in the presence of synaptic blockers (see section 2.1 for details of synaptic blocker application). Since synaptic activity was blocked, it

was possible to record intrinsic responses of MEC layer II SCs. This allowed the isolation of activity on a single-cell level without the influence of the network, present *in-vivo*. This isolation is important because the post-stimulus delay firing recorded from the EC *in-vivo* may have been influenced by the various interconnections of the EC with other MTL regions (see Figure 1.2 for MTL circuitry). Indeed, various models have proposed that post-stimulus sustained firing activity may be driven by network properties (Wang, 2001). By blocking synaptic transmission, we were able to examine if SCs can exhibit post-stimulus (i.e. after the depolarizing current pulse) firing without the influence of the network. Brief depolarizing current pulses evoked a burst of action potentials, which exhibited adaptation of the spike-frequency (Figure 1.3C top - Khawaja and Alonso, 2005 unpublished data). Although various cortical neurons express currents (i.e. afterhyperpolarization (AHP) currents - discussed in detail in section 1.4.1 - 1.4.2 below) that underlie spike-frequency adaptation (SFA), it is not known if these currents exist in SCs. The spike burst was followed by an AHP (discussed in detail in section 1.4.1 - 1.4.2 below), after which the membrane potential returned to baseline (i.e. firing terminated). This is not surprising since currents (i.e. AHP currents - discussed in detail in section 1.4.1 - 1.4.2 below) that underlie SFA and cause post-burst spike termination may be present in SCs, as they are present in various other cortical neurons.

### *1.3.3) MEC layer II SCs exhibit post-burst after-discharges in carbachol*

*In-vivo* studies have shown that EC neurons from superficial layers exhibit post-stimulus firing during the delay period of WM tasks (section 1.2.6). As discussed in the last section (section 1.3.2), a brief depolarizing current pulse (i.e. lasting 1 sec) evokes an adapting spike-burst in SCs, which may be terminated due to various currents (i.e. AHP

currents - discussed in detail in section 1.4.1 - 1.4.2 below) that enable the burst to adapt. However, in the presence of carbachol, a cholinergic muscarinic receptor agonist, MEC layer II SCs exhibit pulse-evoked post-burst after-discharges (Figure 1.3B top - Khawaja and Alonso, 2005 unpublished data; Magistretti et al., 2004) after termination of the pulse. As observed in EC neurons exhibiting post-stimulus delay firing *in-vivo*, the frequency of the post-burst after-discharges observed in MEC II SCs in *in vitro* slices is greater than the baseline frequency observed before the current pulse. In addition, the duration of the current pulse (i.e. 1 sec) used to trigger the post-burst after-discharges in SCs is comparable to the duration of the stimulus presentation (i.e. 500 ms in Suzuki et al., 1997) during WM tasks (see section 1.2.6). Therefore, the protocol for triggering post-burst after-discharges in whole-cell patch clamp may be used as a cellular model for the post-stimulus delay firing activity exhibited in EC neurons during WM tasks. It has been proposed that the post-burst after-discharges exhibited by SCs may be due to the activation of an NCM (non-specific cationic muscarinic) current (Magistretti et al., 2004), which is enabled by stimulation of cholinergic muscarinic receptors (i.e. by carbachol). This $Ca^{2+}$-dependent NCM current (i.e. mostly $Na^{+}/Ca^{2+}$ influx through "NCM channels") is activated as the pulse-evoked spike-burst allows $Ca^{2+}$-influx into SCs (Magistretti et al., 2004). However, the specific details of how muscarinic receptors signal the "NCM channel" have not been determined.

### *1.3.4) Post-burst after-discharges in MEC layer II SCs are non-adapting*

An important feature of the pulse-evoked post-burst after-discharges observed in MEC layer II SCs *in-vitro* is their ability to be sustained in a non-adapting manner for tens of seconds after current stimulus termination (Figure 1.3B bottom) (Magistretti et al.,

2004). When the spike-burst was evoked under control conditions in MEC layer II SCs, the spike-frequency adapted (i.e. spike-frequency gradually decreased; Figure 1.3C top). However, after carbachol application, spike frequency increased in SCs (i.e. SFA decreased; Figure 1.3C bottom). Thus, we propose that SCs may contain currents (i.e. AHP currents) underlying SFA and that inhibitory modulation of these currents may permit the non-adapting nature of post-burst after-discharges in these cells. To test this hypothesis, it is important to determine if MEC layer II SCs express currents (i.e. AHP currents) that underlie SFA in SCs and to determine if these currents can be modulated.

## 1.4) Ionic Mechanisms and modulation of SFA

### *1.4.1) SFA*

SFA is a process whereby the electrical activity (instantaneous firing frequency) of a neuron is gradually reduced when it is exposed to a sustained excitatory stimulus (i.e. depolarizing current stimulus) (Hille, 2001). It is generally believed that SFA underlies behavioral habituation observed in sensory systems during a sustained stimulus (Benda et al., 2005). Figure 1.4 shows an example of prominent SFA recorded from a hippocampal CA1 pyramidal neuron (Madison and Nicoll, 1984). The firing rate of these neurons gradually decreases and they stop firing well before the termination of the depolarizing current pulse (Madison and Nicoll, 1984). In addition, application of $Cd^{2+}$, which blocks $Ca^{2+}$-conductances, reduces SFA in CA1 pyramidal neurons (Figure 1.4 top). The bottom traces of Figure 1.4 show an example of the $Ca^{2+}$-dependent post-burst AHP of a CA1 pyramidal neuron. AHP currents activate after action potentials and are known to hyperpolarize the membrane potential during repetitive firing, leading to SFA (Sah, 1996;

Stocker et al., 2004). $Ca^{2+}$-dependent SFA and post-burst AHPs have been observed in many CNS cells such as cortical neurons *in vitro* (Schwindt et al., 1988a; Lorenzon and Foehring, 1992; Barkai and Hasselmo, 1994; Villalobos et al., 2004) and *in vivo* (Ahmed et al., 1998). They have also been observed in PNS cells such as sympathetic ganglion cells (Pennefather et al., 1985), vagal neurons (Sah and McLachlan, 1991) and myenteric neurons (Vogalis et al., 2002). Furthermore, the $Ca^{2+}$-dependent currents underlying SFA and the post-burst AHP are known to be mediated by $K^+$ channels in most neurons (Sah, 1996; Stocker et al., 2004). The previous section provided evidence that suggested the importance of characterizing the ionic mechanisms underlying SFA in MEC layer II SCs (see section 1.3.4). Although MEC layer II SCs appear to exhibit short-term SFA and a post-burst AHP (Alonso and Klink, 1993), their underlying currents have not been determined.

### *1.4.2) Medium and slow AHP currents*

Two different currents underlie the post-burst AHP in numerous cell types, including hippocampal and neocortical cells (Pennefather et al., 1985; Schwindt et al., 1988b; Sah and McLachlan, 1991; Stocker et al., 1999). These are known as the medium AHP current ($mI_{AHP}$) and the slow AHP current ($sI_{AHP}$) (Pennefather et al., 1985; Schwindt et al., 1988b; Sah and McLachlan, 1991; Stocker et al., 1999). $mI_{AHP}$ and $sI_{AHP}$ are known to contribute to the early and late phases of SFA, respectively, in cortical neurons (Lorenzon and Foehring, 1992; Stocker et al., 2004). In addition, $Ca^{2+}$-dependent $K^+$ currents have been shown to contribute to $mI_{AHP}$ and $sI_{AHP}$ in cortical neurons (Stocker et al., 2004). Based on evidence provided earlier (see section 1.3.3 – 1.3.4 for details), it is therefore important to determine if these currents exist in MEC layer II SCs since they

may contribute to SFA in these cells as well. Specifically, it is not known whether MEC layer II SCs contain $mI_{AHP}$ and $sI_{AHP}$ or if $Ca^{2+}$-dependent $K^+$ channels are involved. Therefore, the working hypothesis is that *MEC layer II SCs contain medium and slow $Ca^{2+}$-dependent $K^+$ currents.*

### *1.4.3) $mI_{AHP}$ components*

Generally, $mI_{AHP}$ comprises both voltage-dependent and voltage-independent components while $sI_{AHP}$ is entirely voltage-independent (Sah and Isaacson, 1995; Stocker, 2004; Stocker et al., 2004). For example, the voltage-dependent $K^+$ M-current ($I_M$) (Storm, 1989) and the voltage-dependent $K^+/Na^+$ h-current ($I_h$) (Storm, 1989) contribute to $mI_{AHP}$ in hippocampal neurons. $mI_{AHP}$ is also composed of the $Ca^{2+}$-dependent $K^+$ currents $I_C$ and $I_{AHP}$ (discussed later in section 1.4.4) in hippocampal neurons (Lancaster and Nicoll, 1987). It has been shown that $I_C$ is a voltage-dependent current, while $I_{AHP}$ is voltage independent (Storm, 1990). The trace in Figure 1.5 shows $mI_{AHP}$ and $sI_{AHP}$ in a representative hippocampal neuron, using the whole-cell voltage-clamp technique, after blocking all voltage-dependent currents underlying $mI_{AHP}$ (Stocker et al., 1999; Shah et al., 2002). In this experiment, currents were evoked by applying a +70 mV depolarizing voltage step of 100 ms duration from a holding potential of -50 mV. Such depolarizing voltage steps are known to activate numerous voltage-dependent currents, including calcium-influx through voltage-gated calcium channels (Sah, 1996; Stocker et al., 2004). The block of voltage-dependent currents of $mI_{AHP}$ in hippocampal neurons allowed the isolation of the voltage-independent $Ca^{2+}$-dependent $K^+$ current $I_{AHP}$. The medium duration current decayed much faster (hundreds of milliseconds) and had a much smaller time constant than $sI_{AHP}$ in hippocampal cells (several seconds) (Stocker et al., 2004).

This section has described how it is possible to evoke the various components of $mI_{AHP}$ and how to isolate the $Ca^{2+}$-dependent $K^+$ current underlying $I_{AHP}$ in hippocampal cells. Next, studies which have aimed to reveal the channels that mediate $I_{AHP}$ in various neurons will be described (Sah and Isaacson, 1995; Stocker, 2004; Stocker et al., 2004).

### *1.4.4) Channels underlying $I_{AHP}$*

Experimental work on a variety of neuron types has shown that the voltage-independent $Ca^{2+}$-dependent $K^+$ current ($I_{AHP}$), is mediated by small-conductance (5 – 20 pS) SK channels (Sah and Isaacson, 1995; Stocker, 2004; Stocker et al., 2004). SK channels are expressed in a variety of central and peripheral neurons including EC neurons (Stocker, 2004). Moreover, SK channels $K_{Ca}$ 2.2 and $K_{Ca}$ 2.3 are sensitive to the bee-venom toxin apamin (Stocker, 2004) while $K_{Ca}$ 2.1 channels are apamin-insensitive (D'Hoedt et al., 2004). As shown for a representative hippocampal cell in Figure 1.5, apamin application blocked SK channels and the $I_{AHP}$ component of $mI_{AHP}$, while the apamin-insensitive $sI_{AHP}$ remained unaffected (Stocker et al., 1999). Apamin-sensitive SK channels contribute to $mI_{AHP}$ in the majority of cortical neurons (Stocker et al., 2004). It is important to determine the underlying mechanisms of $mI_{AHP}$ in MEC layer II SCs (see section 1.3.2 – 1.3.3 for explanation). It is not known whether $I_{AHP}$ is a component of $mI_{AHP}$ in MEC layer II SCs; and therefore, it is not known whether apamin-sensitive SK channels contribute to $mI_{AHP}$ in these cells. However, it has been shown that apamin-sensitive SK subunits are expressed in the EC. We therefore hypothesize that *apamin-sensitive SK channels contribute to $mI_{AHP}$ in MEC layer II SCs.*

### *1.4.5) $sI_{AHP}$ characteristics*

As described above, $mI_{AHP}$ is mediated by several different voltage-dependent and voltage-independent conductances (section 1.4.3). In contrast, $sI_{AHP}$ is known to be mediated solely by a calcium-dependent (voltage-independent) $K^+$ conductance in the majority of central nervous system and peripheral nervous system cell types (Sah and Isaacson, 1995; Stocker, 2004; Stocker et al., 2004). $sI_{AHP}$ activates very slowly during action potentials and contributes to the late phase of SFA, thereby controlling repetitive firing and limiting the number of action potentials evoked by a prolonged (> 1 sec) current stimulus (Stocker et al., 2004). In addition, $sI_{AHP}$ activates slowly (~ 500 ms) and its decay time constant ranges from 1 - 4 s (for an example, see the right trace of Figure 1.5) (Stocker et al., 2004). It has also been reported that $sI_{AHP}$ channels, whose molecular nature remains unresolved, have a small single-channel conductance (3 – 7 pS) (Sah, 1996). Although there are no known pharmacological blockers of $sI_{AHP}$ channels (Stocker et al., 2004), $sI_{AHP}$ can be modulated by a number of neurotransmitters and second messenger pathways (Stocker, 2004).

### *1.4.6) Modulation of $sI_{AHP}$ and SFA*

Studies have revealed that several neurotransmitters and second messenger pathways can control SFA by modulating $sI_{AHP}$ in a variety of neuron types (Nicoll et al., 1990). For example, several monoamines, including noradrenaline, serotonin and histamine attenuate $sI_{AHP}$ and SFA in hippocampal cells (Nicoll et al., 1990) via $\beta_1$, 5-$HT_4$-like and $H_2$ receptors, respectively (Madison and Nicoll, 1982; Haas and Greene, 1986; Madison and Nicoll, 1986; Zifa and Fillion, 1992). After being released onto target neurons from the axon terminals of brainstem neurons, these monoamines can

presumably bind to their respective receptors to activate the enzyme adenylate cyclase (Pedarzani and Storm, 1993), which synthesizes 3'-5'-cyclic adenosine mono-phosphate (cAMP), an intracellular second messenger (Nicoll et al., 1990). In hippocampal cells, the effects of cAMP on $sI_{AHP}$ and SFA are mediated by the ubiquitous cAMP-dependent protein kinase (Pedarzani and Storm, 1993), also known as PKA (Nicoll et al., 1990). In hippocampal cells, suppression of SFA and $sI_{AHP}$ may occur by PKA phosphorylation of the $sI_{AHP}$ channel itself or some other intermediary protein or by activating other enzymatic pathways (Nicoll et al., 1990; Pedarzani and Storm, 1993). Previous evidence suggests that it is important to determine if the currents underlying SFA and $sI_{AHP}$ in MEC layer II SCs can be modulated (see section 1.3.4). Also, activation of the cAMP pathway suppresses SFA and $sI_{AHP}$ in hippocampal cells. Based on this evidence, we hypothesize that *inhibitory modulation by activation of the cAMP pathway suppresses SFA and $sI_{AHP}$ in MEC layer II SCs* as well.

It is important to reveal the currents that underlie SFA in MEC layer II SCs (see section 1.3.4 for explanation). Since $mI_{AHP}$ and $sI_{AHP}$ underlie the medium and slow phases of SFA in cortical neurons (section 1.4.2), it is important to establish if these currents exist in MEC layer II SCs and to determine their ionic mechanisms. It is also important to determine if the apamin-sensitive $I_{AHP}$ (section 1.4.4) exists in MEC layer II SCs. In addition, it is important to establish if $sI_{AHP}$ and SFA are modulated by the cAMP pathway in SCs (section above in current section). Although other currents such as $I_M$ and $I_h$ (section 1.4.3) may be components of the $mI_{AHP}$ exhibited in MEC layer II SCs, this thesis will focus on the $Ca^{2+}$-dependent $K^+$ currents that underlie $mI_{AHP}$. As a result, the contribution of other currents (i.e. $I_M$ and $I_h$) to $mI_{AHP}$ or SFA will not be examined in

this thesis. Based on the cumulative evidence presented for various cortical cell types (see section 1.4), including MEC layer II SCs, the following hypotheses are proposed:

1. ***MEC layer II SCs contain medium and slow $Ca^{2+}$-dependent $K^+$ currents.***
2. ***Apamin-sensitive SK channels contribute to $mI_{AHP}$ in MEC layer II SCs.***
3. ***Inhibitory modulation by activation of the cAMP pathway suppresses spike-frequency adaptation and $sI_{AHP}$ in MEC layer II SCs.***

In the remainder of the thesis, I will describe experiments that were performed to validate or invalidate these hypotheses. In the next chapter I describe the procedures and materials that were used to perform these experiments and to analyze the data obtained.

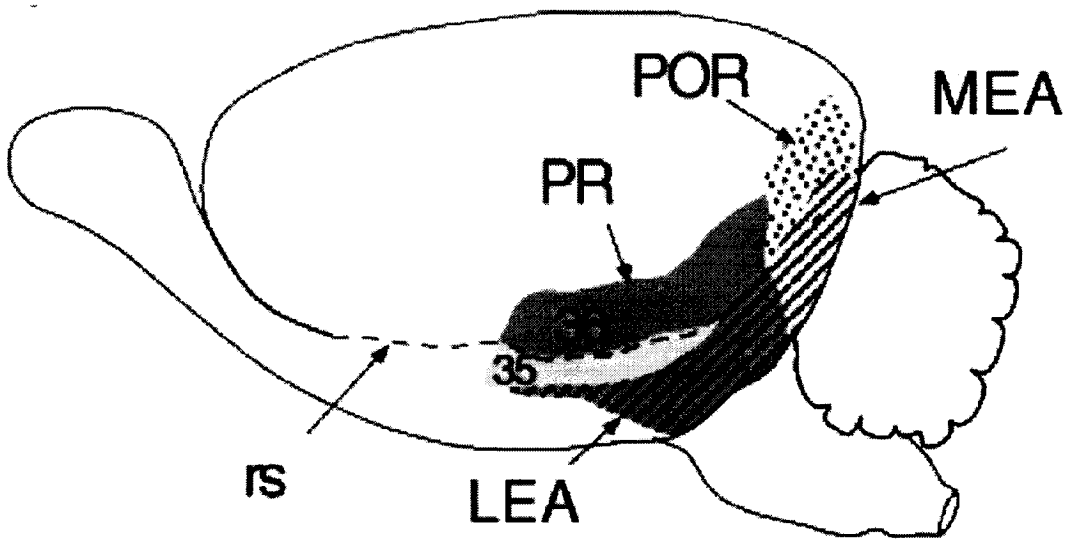


**Figure 1.1 Location of the EC**. Lateral view of the rat brain in which several areas of the MTL are shown. These include the medial entorhinal area/cortex (MEA or MEC; light hatched pattern), the lateral EC/area (LEA or LEC; dark hatched pattern), the perirhinal cortex (PR; areas 35 (light gray) and 36 (dark gray)) and postrhinal cortex (POR; mottled shading pattern). rs, rhinal sulcus.

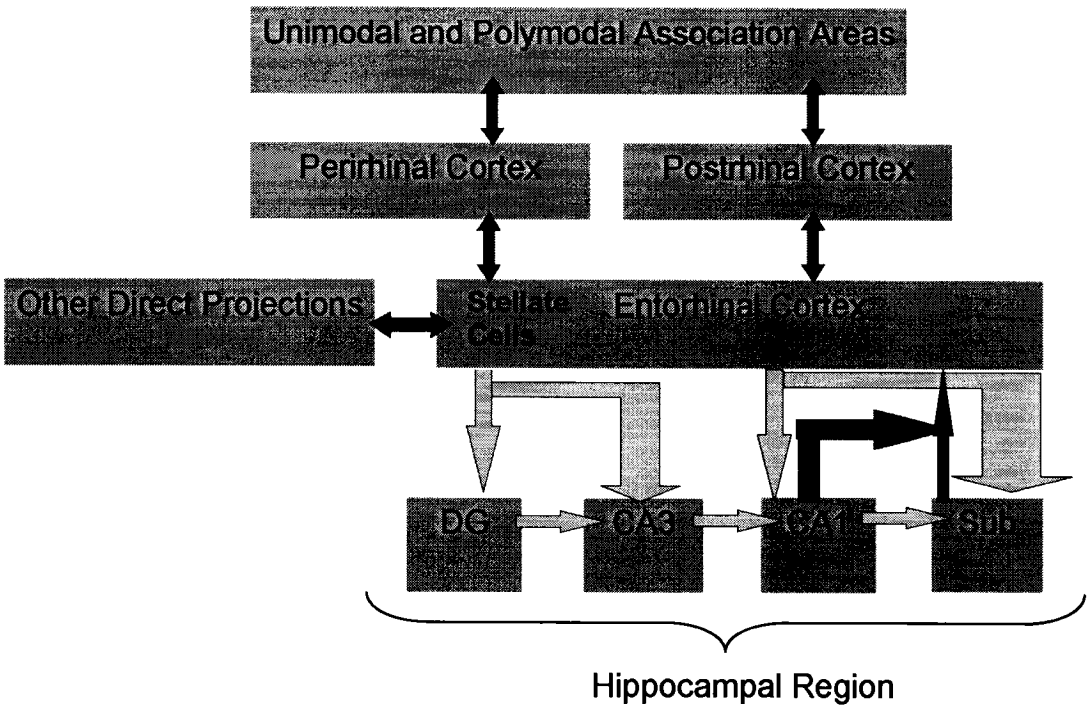


**Figure 1.2 MTL circuitry**. Schematic view of MTL circuitry and other brain areas interconnected to the MTL. DG (dentate gyrus); Sub (subiculum); CA3 and CA1 are two of the CA fields of the hippocampus.

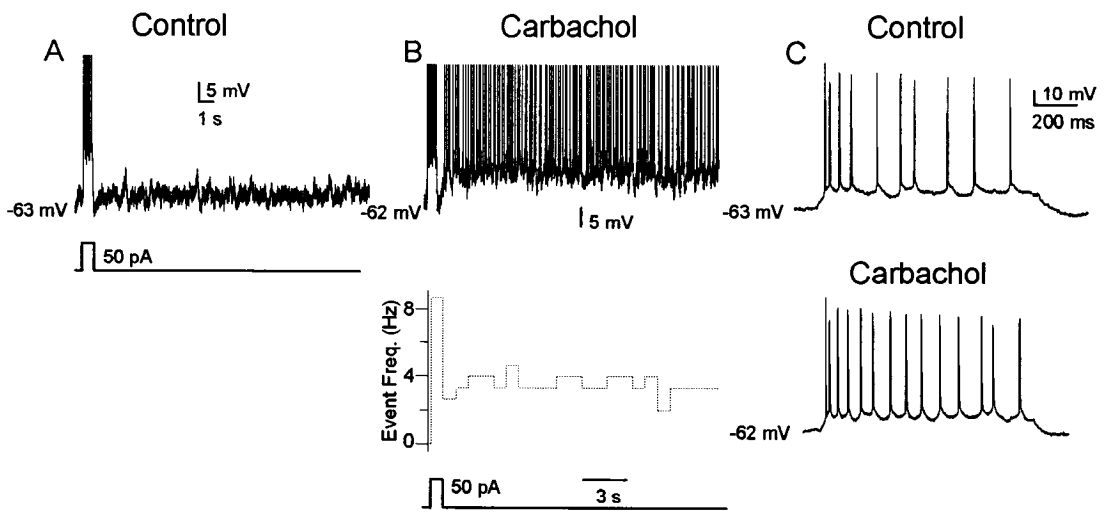


**Figure 1.3 Non-adapting post-burst after-discharges in MEC layer II SC**. *A*, Voltage response of a representative MEC layer II SC evoked by a 50 pA depolarizing current pulse of 1 s duration. *B*, Voltage response showing post-burst after-discharges in response to the same pulse delivered in the presence of 10 μM carbachol (top) and the corresponding frequency graph (bottom) using a bin of 2.4 s. *C*, Voltage responses during the current stimulus before (top) and after (bottom) 10 μM carbachol application.

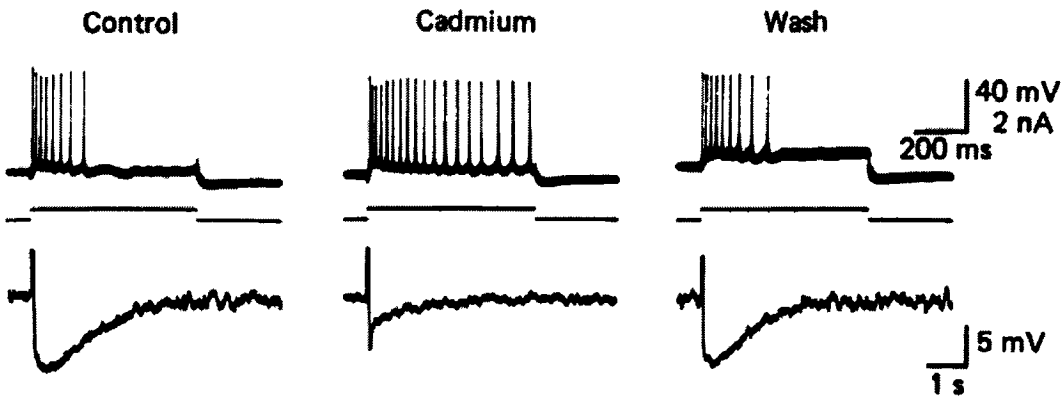


**Figure 1.4. SFA and the post-burst AHP.** *Top,* Voltage responses of a representative hippocampal CA1 pyramidal neuron evoked by a 0.5 nA depolarizing current pulse of 650 ms duration showing SFA under control conditions (left), after application of 100 μM $Cd^{2+}$ (middle) and after washout of drug (right). *Bottom,* Voltage responses (same neuron as in *A*) evoked by a depolarizing current pulse of 60 ms duration showing the effect of 100 μM $Cd^{2+}$ on the AHP.

Reprinted with the permission of Madison DV, Nicoll RA (1984) Control of the repetitive discharge of rat CA 1 pyramidal neurones in vitro. J Physiol 354:319-331. (see Appendix 1.2)

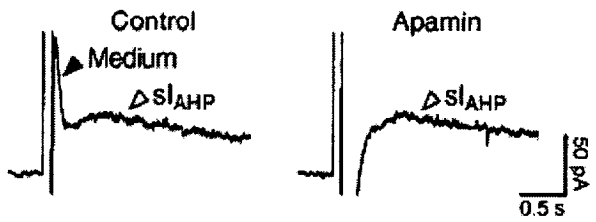


**Figure 1.5. Apamin-sensitivity of $I_{AHP}$ in hippocampal CA1 pyramidal neurons.** Current responses of a representative hippocampal CA1 pyramidal neuron evoked by a +70 mV depolarizing voltage step of 100 ms duration from a holding potential of -50 mV showing $I_{AHP}$ and $sI_{AHP}$ under control conditions (left) and after application of 50 nM apamin (right). Note that $I_{AHP}$ (blocked by apamin) is absent from the right trace.

Reprinted with the permission of Stocker M, Krause M, Pedarzani P (1999) An apamin-sensitive Ca2+-activated K+ current in hippocampal pyramidal neurons. Proc Natl Acad Sci U S A 96:4662-4667. Copyright © 1999 by The National Academy of Sciences (see Appendix 1.3)

# CHAPTER 2: Materials and Methods

## 2.1) Rat *in-vitro* slice preparation

All experimental procedures involving animals were performed in accordance with a protocol approved by the McGill University Animal Care Committee. Male Long-Evans (L.E.) rats (P21 – P25) (Charles River, QC) were used for all experiments. Initially, the rat was anesthetized, through intra-peritoneal (I.P.) injection, with a sub-lethal dose of ketamine/xylazine (0.3 mL/250 g). After deep anesthesia, intra-cardiac perfusion (~15 – 25 mL) was performed with ice-cold (~ 4 °C) perfusing solution through the left ventricle while a cut was made in the right atrium. The perfusing solution was maintained at pH 7.4 by saturation with 95% $O_2$ – 5 % $CO_2$ and it consisted of (in mM): 110 choline chloride, 1.25 $NaH_2PO_4$, 2.5 KCl, 0.5 $CaCl_2$, 7 $MgCl_2$, 25 $NaHCO_3$, 3 sodium pyruvate, 1.3 ascorbic acid and 7 glucose. The perfusing procedure allowed the brain to become very cold, thereby reducing the risk of anoxia, which may have occurred otherwise. In addition, the perfusing solution was a choline-based solution with a high concentration of $MgCl_2$. This limited the excitability of the slice, thus keeping the slice healthy during cutting procedures. The rat was then decapitated and the brain was quickly removed from the cranium and placed in ice-cold (~ 4 °C) perfusing solution (mentioned above). 350 μM horizontal slices, consisting of the MEC, LEC, the hippocampal region and part of the PR, were excised using a vibratome (Leica VT1000 S, Wetzlar, Germany). Slices were subsequently transferred to an incubation chamber and were submerged for 1 – 1.5 hours at room temperature (~ 22 °C). The solution used for incubation (pH 7.4 by saturation with 95% $O_2$ – 5 % $CO_2$) contained (in mM): 126 NaCl, 25 $NaHCO_3$, 2.5 KCl, 2 $CaCl_2$, 2 $MgCl_2$ and 10 glucose. The artificial cerebrospinal fluid

(ACSF) used for recording was identical to the incubation solution except for the addition of kynurenic acid (2 mM) and picrotoxin (100 μM) to block glutamatergic and GABAergic synaptic transmission, respectively. For recording, individual slices were transferred to the recording chamber, where they were submerged and perfused with ACSF (rate 2 mL/min) at room temperature (~ 22 °C). Slices were kept 5 - 6 hours for recording.

## 2.2) Drugs and channel blockers

Stock solutions of 300 mM $CdCl_2$ (Sigma, St. Louis, MO), 2 M $CoCl_2$ (Sigma), 30 mM ZD-7288 (Tocris, Ellisville, MO), 20 mM linopirdine dihydrochloride (Tocris) and 1 mM tetrodotoxin (TTX) (Alomone Labs, Jerusalem, Israel) were prepared in doubled-distilled $H_20$. Stock solutions of 50 mM forskolin (Tocris, Ellisville, MO) and 200 mM Ro 20-1724 (Tocris, Ellisville, MO) were prepared in DMSO. Bulk stocks of $CdCl_2$ and $CoCl_2$ were stored at 4 °C, whereas small aliquots of the other drugs were stored at -20 °C. A stock solution of 300 μM apamin (Tocris) was prepared by using 0.1 M acetic acid as the solvent and was stored in individual aliquots at -20 °C. These stock solutions were later diluted in the ACSF and bath applied at the required concentrations.

## 2.3) Whole-cell patch clamp

Whole-cell patch clamp recordings were obtained from MEC layer II SCs and non-SCs. Slices were observed under an upright microscope (Axioscope, Zeiss) equipped with a 4X and a 40X (water immersion) objective as well as a near infrared charge-coupled device camera (XC-75, Sony Corporation). Initially, using the 4X objective,

layer II of the MEC was identified as a thick band of cells extending from the parasubiculum (located medially) to the lateral EC transition zone (Blackstad, 1956). Borosilicate glass capillary tubes (outer diameter 1.5 mm and inner diameter 0.75 mm) (Sutter Instrument, Novato, CA) were pulled on a P97 Flaming-Brown micropipette puller (Sutter Instruments, Novato, CA) to make patch pipettes. These pipettes (resistance 4 – 7 MΩ) were filled with a solution (pH adjusted to pH 7.3 with KOH) containing (in mM): 120 potassium gluconate (Kgluc) or 120 potassium methylsulfate ($KMeSO_4$), 10 *N*-[2-hydroxyethyl] piperazine-*N*'-[2-ethanesulphonic acid] (HEPES), 0.2 ethylene glycol-bis (β-aminoethyl ether) *N,N,N',N'*-tetraacetic acid (EGTA), 7 diTris-phosphocreatine, 20 KCl, 2 $MgCl_2$, 4 $Na_2$ adenosine tri-phosphate, 0.3 Tris guanosine tri-phosphate and 0.1% biocytin. During recording, SCs and non-SCs were tentatively distinguished based on differential electrophysiological properties (i.e. SC have a larger hyperpolarization-induced depolarizing sag (HS) and rebound potential (RP) than non-SCs), as described previously (Alonso and Klink, 1993). Cell type was confirmed later by histo-chemical processing (see section 2.8).

Giga-seals (> 1GΩ) were formed on principal cells (i.e. SCs or non-SCs) and the underlying membrane patches were ruptured by applying suction. All whole-cell recordings were obtained using an Axopatch 200B amplifier (Axon Instruments, Union City, CA). Signals were low-pass filtered at 2 kHz (-3 dB) and were digitally sampled at 5 kHz during current-clamp recordings. Signals were low-pass filtered at 1 kHz (-3 dB) and were digitally sampled at 2 kHz during voltage-clamp recordings. An external homemade signal generator (MNI, McGill) or the Digidata 1200 was used to deliver pulses. Clampex 8.0 (Axon Instruments) and the Digidata 1200 were used for data acquisition on a Pentium I computer. Averaging, digital subtractions, fittings and other

statistical analyses were performed using Clampfit 9.0 (Axon Instruments) and Origin (Microcal, Northampton, MA). In current-clamp experiments, all cells used for analysis had spike amplitudes > 60 mV and series resistance < 30 MΩ. In voltage clamp experiments, the series resistance was compensated at 40% with a 10 μs lag. Errors caused by liquid-junction potentials were not corrected for.

## 2.4) Electrophysiological protocols used to evoke HS, RP, post-burst AHP, AHP currents and SFA

HSs and RPs were evoked in SCs by applying 100 pA hyperpolarizing pulses lasting 600 ms. The resting membrane potential (RMP) was near –62 mV in SCs and was adjusted by DC current injection if needed. Actual averaged baseline values achieved during these experiments were -63 ± 0.9 mV ($Gluc^-$) and -62 ± 1 mV ($MeSO_4^-$). Spike-trains and post-burst AHPs were evoked using 160 pA depolarizing pulses lasting 1 sec, or 150 pA pulses lasting 6 sec. Short pulses (1 sec) were applied after the RMP was adjusted by DC current injection to a value near –55 mV (averaged values obtained experimentally were -57 ± 1.5 mV ($Gluc^-$) and -54 ± 1.5 ($MeSO_4^-$). When longer (6 sec) pulses were used, the RMP was adjusted by DC current (to -60 ± 1 mV). Voltage-clamp recordings were obtained, from a holding potential of -50 mV, by first applying a -20 mV step hyperpolarization of 500 ms duration to observe the activation of h-current ($I_h$), a hyperpolarization-activated depolarizing non-selective cationic conductance (Hille, 2001), and then a +70 mV step depolarization of 100 ms duration to induce the medium and slow AHP currents.

## 2.5) Electrophysiological protocols used to reveal the reversal potentials of $mI_{K(Ca)}$ and $sI_{AHP}$

To determine the reversal potential of $mI_{K(Ca)}$ and $sI_{AHP}$, leak currents were first evoked by applying a step hyperpolarization lasting 16 s to potentials ranging from -60 to -115 mV, from a holding potential of -50 mV. Next, $mI_{K(Ca)}$ and $sI_{AHP}$ were evoked by applying a 500 ms step depolarization to +20 mV followed by a step to test voltages ranging from -50 mV to -115 mV. The leak currents were subtracted from the depolarizing pulse-evoked currents to extract $sI_{AHP}$ and $mI_{K(Ca)}$. The $sI_{AHP}$ amplitude was measured (relative to baseline) at the time when the current was at its peak. The amplitude of $mI_{K(Ca)}$ was measured 20 ms after the end of the depolarizing pulse in order to reduce the confounding effects of the inward capacitive transients present in the current traces when we stepped from the conditioning voltage (+20 mV) to test voltages below the holding potential (-50 mV). In addition, the decay time constant of $mI_{K(Ca)}$ was 40 ms and $sI_{AHP}$ activated very slowly in MEC layer II SCs. Therefore, the measurement of the current at 20 ms was mostly $mI_{K(Ca)}$. The Nernst potential for various ions was determined using the equation:

$$E_x = (RT / zF) * \ln ([X]_o / \ln [X]_i)$$

Here, x is the ion, z is its valence, R is the gas constant, T is the temperature (in K), F is Faraday's constant, $[X]_o$ is the concentration of the ion in the extracellular perfusing solution and $[X]_i$ is the concentration of the ion in the intracellular pipette solution.

## 2.6) Measurement of HS%, RP, SFA index and post-burst AHP area

The HS%, an index of $I_h$ magnitude, was calculated as the percent change of the baseline membrane potential from peak (~20 mV) to steady state during the pulse. The RP was calculated as the peak voltage deflection observed after the termination of the hyperpolarization pulse. The adaptation indices were defined to be $100 * (1 - (F_{ad} / F_1))$ where $F_{ad}$ was the instantaneous spike frequency between the final two action potentials in the spike-train and $F_1$ was the instantaneous spike frequency between the first two action potentials. The SFA index was arbitrarily defined to be 100 if the cell stopped firing $\leq$ 500 ms before the end of the current stimulus. The post-burst AHP area for the short pulse (1 sec duration) was measured as the area below baseline between the end of the spike-train and the end of the sAHP (the sAHP is indicated by an arrow in Figure 2B).

## 2.7) Measurement of the amplitudes and time constants of $mI_{AHP}$, $mI_{K(Ca)}$ and $sI_{AHP}$

In all experiments except for the reversal potential experiments, the amplitudes and time constants of $mI_{AHP}$, $mI_{K(Ca)}$ and $sI_{AHP}$ were obtained by doing exponential fittings of the current traces. With intracellular $Gluc^-$, a bi-exponential fitting was applied to obtain the amplitude and time constant of $mI_{K(Ca)}$ (A1 and Tau1). The $sI_{AHP}$ amplitude and time constant were obtained by doing a mono-exponential fitting from Tau1 * 4 until the end of the current response. On the other hand, due to the detectable peak of $sI_{AHP}$ with intracellular $MeSO_4^-$, a mono-exponential fitting was required for each current component. For these cells, $mI_{K(Ca)}$ or $mI_{AHP}$, and $sI_{AHP}$ were fitted from their respective peaks to their respective antipeaks. Note that a small number of cells did not have a clear

$sI_{AHP}$ peak with intracellular $MeSO_4^-$. For these cells, the time of the $sI_{AHP}$ peak was taken to be the mean time of the $sI_{AHP}$ peak of those cells in which the $sI_{AHP}$ peak was detectable.

## 2.8) Histo-chemical processing of EC slices

After completion of the electrophysiological protocols, the slices were fixed with 4% paraformaldehyde in 0.1 M sodium phosphate buffer solution (NaPB) and kept at 4 °C. Slices were removed from fixative solution and rinsed in 0.1 M NaPB (3 X 5 minutes). To suppress endogenous peroxidase activity, slices were incubated in 2% $H_2O_2$ in 0.1 M NaPB for 30 minutes. Then, slices were rinsed in 0.1 M NaPB (3 X 5 minutes). Next, the slices were incubated in NaPB/Gelatin (0.2 %)/Triton (0.25 %) for 30 minutes to block non-specific binding sites. The slices were then washed in the Avidin : Biotinylated enzyme complex (ABC) (Vector Laboratories, Burlingame, CA) (with peroxidase as the enzyme) overnight. Slices were thoroughly rinsed the following day. In particular, the washes consisted of the following: first wash (4 x 1 minute), second wash (1 x 30 minutes) followed by 6 more washes, one every hour. On the third and final day, slices were first rinsed (3 x 10 minutes) in 0.1 M Tris Buffered Saline (TBS). Next, the slices were transferred to a solution containing the enzyme substrate 3, 3'-diaminobenzidine (DAB) to localize peroxidase. The DAB solution also contained $Ni^{2+}$, which changed the staining color from brown to gray/black and intensified the reaction of the DAB solution with peroxidase. This reaction was stopped once the preferred amount of staining was obtained by washing the slices in TBS (3 x 10 minutes). Once the slices were dry, heated moviol (Calbiochem, La Jolla, CA) was used to mount them on glass

cover slides. The slides were then cover-slipped and kept in a dark room overnight. The next day, slices were observed with a Nikon microscope (Eclipse E800) under 20x magnification to determine the location and type of cells that were recorded and photographs were obtained. A small number of cells were not detectable; and therefore, electrophysiological characteristics were used to identify them. In particular, SCs and non-SCs were differentiated based on the amount of evoked HS (i.e. SC have a larger HS than non-SCs - see section 2.4, 2.6 for details on HS). Thus, the use of both histo-chemical and electrophysiological approaches enabled us to confirm that most recordings were obtained from cells in layer II of the MEC. In addition, it enabled use to identify the type of principle cell recorded. In a few cases when either the recordings were not obtained from MEC layer II or if the revealed neuron was not a principal cell, recordings were excluded from analysis.

## 2.9) Statistical analysis

Paired and unpaired Student's t tests were used. In particular, unpaired Student's t tests were used to analyze the differential effects of intracellular $Gluc^-$ and $MeSO_4^-$. For all other statistical analysis, paired Student's t tests were used. The p values used for significance were: $*p < 0.05$, $**p < 0.01$, $***p < 0.001$. Also, averaged data were represented as mean ± S.E.M. throughout the thesis.

# CHAPTER 3: Effects of intracellular anions on MEC layer II SCs

## 3.1) Intracellular anions differentially affect ionic conductances in hippocampal cells

As outlined in the hypotheses (section 1.4.6), the objective of this thesis is to uncover the currents underlying SFA and to determine how these currents can be modulated in MEC layer II SCs. However, previous studies using the whole-cell patch clamp technique have shown that the currents underlying SFA, as well as other currents, may be affected by the composition of the intracellular pipette solution (Zhang et al., 1994; Velumian et al., 1997). Movement of solutes from the patch pipette into the cell (and vise-versa) during the "washout" period may affect these currents in hippocampal cells (Zhang et al., 1994; Velumian et al., 1997). Therefore, it was important to first reveal if these currents depend on the intracellular pipette solution in MEC layer II SCs as well.

In hippocampal cells, KGluc and $KMeSO_4$, both commonly used as major salts for the patch clamp recording pipette solution, differentially affect several ionic conductances (Zhang et al., 1994; Velumian et al., 1997). Velumian et al., (1997) replaced the internal pipette solution during whole-cell patch clamp recording (i.e. KGluc-based solution replaced by a $KMeSO_4$-based solution and vice-versa) of hippocampal neurons. This allowed them to demonstrate reversible effects of these pipette solutions on various ionic conductances (Velumian et al., 1997). In particular, they applied hyperpolarizing current pulses to evoke $I_h$ (see section 2.4) and showed that $I_h$ is reduced upon replacement of a $MeSO_4^-$-based intracellular pipette solution with a $Gluc^-$-based solution in the recording

electrode. Also, the mAHP and sAHP (section 1.4.1) were both smaller when hippocampal cells were patched with electrodes containing $Gluc^-$. Moreover, $sI_{AHP}$ and SFA (section 1.4.5) were smaller in hippocampal cells patched with a $Gluc^-$-based internal solution. However, both $sI_{AHP}$ and SFA could be restored in hippocampal cells after replacement of the $Gluc^-$-based solution with a $MeSO_4^-$-based solution (Zhang et al., 1994; Velumian et al., 1997). Based on these results from hippocampal cells, we tested if intracellular $Gluc^-$ and $MeSO_4^-$ differentially affect AHP currents, SFA and $I_h$ in MEC layer II SCs.

## 3.2) Effect of intracellular $Gluc^-$ and $MeSO_4^-$ on $I_h$-dependent sag

Previous studies in medial entorhinal cortex (MEC) layer II SCs have shown that the hyperpolarization-induced depolarizing sag (HS) is dependent mostly on $I_h$ activation (Alonso and Klink, 1993; Klink and Alonso, 1993; Dickson et al., 2000). Therefore, measurement of the HS may be used as an index of evoked $I_h$ in these cells (Dickson et al., 2000). Another parameter used to quantify the amount of evoked $I_h$ is the rebound potential (RP) observed after termination of the current stimulus (Alonso and Klink, 1993; Klink and Alonso, 1993; Dickson et al., 2000). Based on previous studies which compared the differential effects of intracellular $Gluc^-$ and $MeSO_4^-$ on $I_h$ in hippocampal cells (Velumian et al., 1997), we hypothesized that MEC layer II SCs would also exhibit a smaller $I_h$-dependent sag with intracellular $Gluc^-$. To test this, we applied a 100 pA hyperpolarizing current pulse lasting 600 ms to evoke a HS and RP. The mean RMP was near –62 mV and was adjusted by DC current injection if needed (-63 ± 0.9 mV ($Gluc^-$) and -62 ± 1 mV ($MeSO_4^-$)). The mean HS%s (see section 2.6 for calculation of HS%s) in

SCs were significantly larger in the $Gluc^-$ group (38 ± 2 % with $Gluc^-$ (n = 14; e.g. Figure 3.1A left) vs. 25 ± 3 % with $MeSO_4^-$ (n = 20; e.g. Figure 3.1A right); p = 0.002). Also, the mean RPs (see section 2.6 for calculation of RP) in SCs were larger in the $Gluc^-$ group (6.3 ± 1 mV with $Gluc^-$ vs. 3 ± 0.9 mV with $MeSO_4^-$; p = 0.02). These results indicate that larger $I_h$ is evoked in SCs when KGluc is used as the major salt component of the intracellular solution. Next, we tested in SCs if intracellular $Gluc^-$ and $MeSO_4^-$ have different effects on SFA as well.

## 3.3) Differential effect of intracellular $Gluc^-$ and $MeSO_4^-$ on SFA

Previous studies have shown that smaller SFA is evoked in hippocampal pyramidal neurons when $Gluc^-$ is the major anion in the intracellular pipette solution compared with $MeSO_4^-$ (see section 3.1). Based on this, it was hypothesized that smaller SFA would also be evoked in MEC layer II SCs patched with a $Gluc^-$-based pipette solution. To test this hypothesis, a spike-train (burst) was evoked by applying a 160 pA depolarizing current pulse lasting 1 second. The RMP was near –62 mV and was adjusted by DC current injection (-57 ± 1.5 mV ($Gluc^-$) and -54 ± 1.5 ($MeSO_4^-$)). The mean SFA index, used to quantify the amount of SFA (see section 2.6 for calculation of SFA index), was significantly smaller in the KGluc group (76 ± 2 with $Gluc^-$ (n = 4; e.g. Figure 3.2A top) and 93 ± 3 with $MeSO_4^-$ (n = 7; e.g. Figure 3.2A bottom); p = 0.01). In addition, firing terminated (i.e. SFA index = 100; section 2.6 for definition of 100% SFA) in 4 out of 7 SCs, recorded with electrodes containing $MeSO_4^-$, before the end of the current stimulus lasting 1 sec. On the other hand, all cells patched with electrodes containing $Gluc^-$ continued firing throughout the current pulse. These results indicated

that intracellular $Gluc^-$ may somehow reduce SFA in SCs. Next, we tested if intracellular $Gluc^-$ and $MeSO_4^-$ can differentially affect the post-burst AHP in MEC layer II SCs.

## 3.4) Differential effect of intracellular $Gluc^-$ and $MeSO_4^-$ on the post-burst AHP

The post-burst AHP was smaller in hippocampal cells patched with electrodes containing $Gluc^-$ compared to when $MeSO_4^-$ was used (section 1.4.1). Based on this, we tested if the post-burst AHP was also smaller in SCs patched with electrodes containing $Gluc^-$. Indeed, the mean post-burst AHP area was significantly smaller in SCs patched with a $Gluc^-$-based solution (5.7 ± 0.7 mV * s with $Gluc^-$ (n = 4; e.g. Figure 3.2C top) vs. 13 ± 0.7 mV * s with $MeSO_4^-$ (n = 7; e.g. Figure 3.2C bottom); p = 0.0001). Based on this data, we concluded that a smaller post-burst AHP is evoked in SCs patched with pipettes containing intracellular $Gluc^-$, a result consistent with previous studies of hippocampal pyramidal cells (section 3.1). Next, we characterized the currents which may mediate the mAHP and sAHP in MEC layer II SCs (Alonso and Klink, 1993) and compared the effects of intracellular $Gluc^-$ and $MeSO_4^-$ on these currents.

## 3.5) Differential effects of intracellular $Gluc^-$ and $MeSO_4^-$ on $mI_{K(Ca)}$ and $sI_{AHP}$

It has been shown previously that hippocampal and neocortical cells contain both medium and slow decaying AHP currents that contribute to SFA (section 1.4.2). According to the first hypothesis (see section 1.4.6 hypothesis 1), it was important to determine if layer II SCs contain medium and slow AHP currents as well. The current

underlying the mAHP is composed of voltage-dependent and voltage-independent components (section 1.4.3) while the sAHP is solely a $Ca^{2+}$-dependent $K^+$ conductance in most cortical neurons (section 1.4.5). In our experiments with MEC layer II SCs, 1 μM TTX was applied to block $Na^+$ channels (Kao, 1972). In addition, to block voltage-dependent components that may contribute to $mI_{AHP}$ (section 1.4.3) in MEC layer II SCs, 20 μM linopirdine and 30 μM ZD-7288 were applied to block $I_M$ (Schnee and Brown, 1998) and $I_h$ (BoSmith et al., 1993), respectively. To evoke both $mI_{K(Ca)}$ and $sI_{AHP}$ in SCs, we applied a 100 ms step depolarization to +20 mV from a holding potential of -50 mV. From this protocol, it was established that SCs exhibit outward currents mediating $mI_{K(Ca)}$ and $sI_{AHP}$ (e.g. Figure 3.3A for $sI_{AHP}$ and Figure 3.3B for $mI_{K(Ca)}$ for each intracellular pipette solution). In addition, $sI_{AHP}$ usually has a well-defined peak (arrow in 3.3A bottom) in SCs patched with a $MeSO_4^-$-based intracellular solution. In particular, out of 16 SCs analyzed under control conditions (TTX/ZD 7288/linopirdine) when intracellular $MeSO_4^-$was in the recording electrode, 14 had detectable $sI_{AHP}$ peaks. On the other hand, $sI_{AHP}$ peaks were not detectable in any of the 7 SCs patched with electrodes containing $Gluc^-$ (e.g. Figure 3.3A top). These results established that MEC layer II SCs express medium and slow AHP currents, whose amplitudes may be differentially affected by $Gluc^-$ and $MeSO_4^-$. The next series of experiments aimed to reveal if these currents were $Ca^{2+}$-dependent.

## 3.6) The $Ca^{2+}$-dependent $sI_{AHP}$ and $mI_{K(Ca)}$

It was important to reveal if $mI_{K(Ca)}$ and $sI_{AHP}$ were $Ca^{2+}$-dependent in MEC layer II SCs. To evoke $mI_{K(Ca)}$ and $sI_{AHP}$, we applied a 100 ms depolarizing voltage step to +20

mV from a holding potential of -50 mV in the presence of 1 μM TTX, 20 μM linopirdine and 30 μM ZD-7288. 300 μM $Cd^{2+}$ and 2 mM $Co^{2+}$ were applied to SCs to block $Ca^{2+}$ conductance in these cells (Klink and Alonso, 1993). Amplitudes and time constants of $mI_{K(Ca)}$ and $sI_{AHP}$ were obtained through exponential fittings (see section 2.7 for details) of these currents before and after $Ca^{2+}$-conductance block. From this, we were able to determine if $Ca^{2+}$-dependent currents are a significant component of $mI_{K(Ca)}$ and $sI_{AHP}$ in MEC layer II SCs. The $sI_{AHP}$ amplitude significantly decreased (by 76 ± 6%) after $Cd^{2+}/Co^{2+}$ application when SCs were patched with pipettes containing $Gluc^-$ (14 ± 3 pA to 2.7 ± 0.85 pA; n = 7; p = 0.009; e.g. Figure 3.4A) and also decreased (by 91 ± 4%) when $MeSO_4^-$ was used (54 ± 17 pA to 2.3 ± 0.4 pA; n = 7; p = 0.02; e.g. Figure 3.4B). Furthermore, $mI_{K(Ca)}$ amplitude significantly decreased (by 68 ± 7%) after $Cd^{2+}/Co^{2+}$ application when SCs were patched with pipettes containing a $Gluc^-$-based internal solution (125 ± 10 pA to 37 ± 6 pA; n = 7; p = 0.0006; e.g. Figure 3.5A) and also decreased (by 58 ± 7%) when $MeSO_4^-$ was used (218 ± 26 pA to 81 ± 14 pA; p = 0.009; e.g. Figure 3.5B). The mean time constants of $mI_{K(Ca)}$ were not significantly different after $Cd^{2+}/Co^{2+}$ application when SCs were patched with electrodes containing either $Gluc^-$ (56 ± 4 ms to 65 ± 5 ms; p = 0.14) or $MeSO_4^-$ (40 ± 2.4 ms to 47 ± 1.9 ms; p = 0.09). Although further studies will be required to establish if the unblocked $mI_{K(Ca)}$ is residual $Ca^{2+}$-dependent current or a different conductance, we can conclude from our results that a significant portion of $mI_{K(Ca)}$ and $sI_{AHP}$ was $Ca^{2+}$-dependent in the presence of each of the intracellular solutions. These studies revealed that MEC layer II SCs contain medium and slow $Ca^{2+}$-dependent currents; and therefore, provided partial support for the first hypothesis.

## 3.7) Discussion

### *3.7.1) Differences in evoked HS and RP in SCs patched with a $Gluc^-$- or $MeSO_4^-$-based pipette solution*

The HS can be used as an index to measure $I_h$ activation in hippocampal pyramidal cells (section 3.1) and MEC layer II SCs (section 3.2). Velumian et al., 1997 reported differences in evoked HSs between hippocampal cells patched with electrodes containing $Gluc^-$ and those containing $MeSO_4^-$. However, HSs were not quantified in that study; and therefore, differences in $I_h$ activation between pipette solutions were based on qualitative analysis. On the other hand, in the present experiments on MEC layer II SCs (section 3.2), both HS%s and RPs were used as a quantitative measure of $I_h$ activation. It was determined that both parameters were significantly larger when cells were patched with electrodes containing $Gluc^-$ than with those containing $MeSO_4^-$. It was now important to determine whether $I_h$ is activated normally in SCs patched with a $Gluc^-$- or a $MeSO_4^-$-based internal solution. Intracellular sharp electrode recording is believed to reveal more physiological responses in hippocampal neurons than whole-cell patch clamp recording (Zhang et al., 1994; Velumian et al., 1997). Therefore, it was useful to compare the HS%s evoked in SCs using sharp electrodes with the HS%s evoked with a $Gluc^-$- or $MeSO_4^-$based pipette solution (see section 3.2). Indeed, previous studies using intracellular sharp electrodes have reported mean HS%s in MEC layer II SCs (Alonso and Klink, 1993). The procedure used for calculating HS%s in these sharp electrode experiments was identical to the procedure we used (see section 2.6 for calculation of HS%s). The HS%s obtained from sharp electrode studies were closer to the mean HS%s in SCs patched with electrodes containing a $MeSO_4^-$-based pipette solution than when

$Gluc^-$ was in the pipette. This indicates that $I_h$ may be potentiated in SCs patched with a $Gluc^-$-based internal solution. Thus, based on our data and the results of previous studies of MEC layer II SCs using sharp electrodes, it can be concluded that $I_h$ is activated normally when $MeSO_4^-$ is used in the intracellular pipette solution during whole-cell patch clamp recording.

### *3.7.2) Differences in evoked SFA in SCs patched with a $Gluc^-$- or $MeSO_4^-$-based pipette solution*

It has been shown that smaller SFA is evoked in hippocampal neurons when intracellular $Gluc^-$ is in the pipette solution than when $MeSO_4^-$ is used (Zhang et al., 1994). In addition, it was reported that SFA undergoes a rapid "rundown" when hippocampal cells are patched with pipettes containing a $Gluc^-$-based internal solution (Zhang et al., 1994). From this, Zhang et al., 1994 concluded that SFA is best preserved when hippocampal cells are patched with $MeSO_4^-$-containing electrodes. As mentioned before, spike-trains were evoked in MEC layer II SCs by using a 160 pA depolarizing current pulse lasting 1 second (section 3.3). From this experiment, it was revealed that SFA was smaller when MEC layer II SCs were patched with $Gluc^-$-containing pipettes (section 3.3). This suggests that intracellular anions may differentially regulate spike patterns in MEC layer II SCs as well. To observe the normal physiology of SCs under control conditions, it is important to determine which intracellular anion evokes normal spike patterns in SCs. Firing terminated in most SCs before the end of the depolarizing current stimulus (described above in this section) when $MeSO_4^-$-containing electrodes were used (section 3.3). On the other hand, SCs exhibited continued firing throughout the current stimulus when patched with pipettes containing a $Gluc^-$-based internal solution

(section 3.3). Prominent SFA, specifically spike termination before the end of the current pulse, has been observed in MEC layer II SCs when intracellular sharp electrodes are used for recording (Alonso and Klink, 1993; Klink and Alonso, 1997a). In particular, Alonso and Klink, 1993 showed that firing terminates in ~ 80% of MEC layer II SCs before the end of depolarizing current stimulus. Thus, we propose that MEC layer II SCs patched with a $MeSO_4^-$-based internal solution may evoke more physiological spike patterns than those patched with pipettes containing $Gluc^-$.

### *3.7.3) Possible basis for the differences in evoked $sI_{AHP}$ in SCs patched with a $Gluc^-$- or $MeSO_4^-$-based pipette solution*

Previous studies compared the effects of intracellular pipette solutions on $sI_{AHP}$ in hippocampal neurons (section 3.1). For example, Velumian et al., (1997) reported that $sI_{AHP}$ is smaller in hippocampal cells patched with electrodes containing $Gluc^-$ than those containing $MeSO_4^-$. The evoked $sI_{AHP}$ (see section 1.4.5 for $sI_{AHP}$ characteristics) was also compared in MEC layer II SCs patched with pipettes containing $Gluc^-$ or $MeSO_4^-$ to determine if they are differentially affected by these intracellular anions. The amplitude of $sI_{AHP}$ was found to be significantly smaller in SCs patched using internal $Gluc^-$ than those patched with a $MeSO_4^-$-based pipette solution, as found in hippocampal neurons. Velumian et al., (1997) proposed that $Gluc^-$ may diffuse into the hippocampal cell during the "wash-out" period and, by somehow affecting $Ca^{2+}$-diffusion, buffering and other actions of $Ca^{2+}$, prevent $Ca^{2+}$ from reaching the channel underlying $sI_{AHP}$. This may account for the differences in $sI_{AHP}$ observed in MEC layer II SCs as well. Another possible explanation is that $Gluc^-$ may have an inhibitory effect on the $Ca^{2+}$-dependent $K^+$

channel underlying $sI_{AHP}$ in MEC layer II SCs. However, additional experiments must be conducted in MEC layer II SCs to confirm or reject these hypotheses.

### *3.7.4) Possible basis for the differences in evoked $mI_{K(Ca)}$ in SCs patched with electrodes containing $Gluc^-$- or $MeSO_4^-$.*

The mechanism by which $Ca^{2+}$ activates the $sI_{AHP}$ channel remains mostly unknown (Stocker et al., 2004). However, much has been revealed in recent years about the mechanisms by which SK channels (small-conductance $Ca^{2+}$-activated $K^+$ channels; see section 1.4.4 for review), are activated in hippocampal cells (Stocker et al., 2004). For example, it is now generally believed that SK channel activation is dependent on the binding of $Ca^{2+}$ to constitutively bound calmodulin (Vogalis et al., 2003; Stocker et al., 2004). In particular, it was shown that $K_{Ca}$ 2.2 activation is associated with the interaction of calmodulin with each of the subunits of $K_{Ca}$ 2.2. In our studies of MEC layer II SCs, it was determined that $mI_{K(Ca)}$ amplitude was significantly lower when cells were patched with pipettes containing $Gluc^-$ than with those containing $MeSO_4^-$ ($p = 0.006$; $n = 7$) . It was also revealed that the $mI_{K(Ca)}$ time constant was greater in SCs patched with pipettes containing a $Gluc^-$-based solution ($p = 0.01$; $n = 7$). Since SK channels contribute to $mI_{K(Ca)}$ in most cortical neurons, they may contribute to $mI_{K(Ca)}$ in MEC layer II SCs as well, as hypothesized (see section 1.4.6 hypothesis 2). If this is true for SCs, it is possible that $Gluc^-$ diffusion into these cells during whole-cell recording may somehow affect the activation of SK channels by $Ca^{2+}$. One possibility is that intracellular $Gluc^-$ may affect the binding of $Ca^{2+}$ to calmodulin, thereby inhibiting the activation of SK channels, and resulting in a smaller $mI_{K(Ca)}$ in SCs patched with electrodes containing a $Gluc^-$-based

pipette solution. However, this is only valid if SK channels contribute to $mI_{K(Ca)}$ in MEC layer II SCs, a hypothesis that will be tested later in the thesis.

### *3.7.5) Specific components of AHP currents are differentially affected by a $Gluc^-$- or $MeSO_4^-$-based pipette solution in SCs*

Velumian et al. (1997) showed that $sI_{AHP}$ is smaller in hippocampal cells patched with a $Gluc^-$-based internal solution. $sI_{AHP}$ was evoked in hippocampal cells patched with a $Gluc^-$- and a $MeSO_4^-$-based pipette solution and was quantified in this study by measuring its area. However, $mI_{AHP}$ was not quantified in this study. As a result, this study did not establish whether $mI_{AHP}$ was differentially regulated by intracellular anions (Velumian et al., 1997). On the other hand, our experiments and quantitative analysis allowed the isolation of the $Ca^{2+}$-dependent currents underlying $mI_{AHP}$ and $sI_{AHP}$ and revealed that both components are smaller in SCs patched with $Gluc^-$ as the major anion in the pipette solution. As far as we know, this is the first time that differential effects of intracellular anions on $mI_{AHP}$ have been shown in neurons.

Although the specific mechanisms underlying the effects of $Gluc^-$- and $MeSO_4^-$-based pipette solutions on $mI_{AHP}$ and $sI_{AHP}$ remain unknown, the present study on MEC layer II SCs revealed that a $MeSO_4^-$-based pipette solution may allow $Ca^{2+}$-dependent $K^+$ currents and SFA to behave in a more natural form during whole-cell patch clamp than when pipettes contain $Gluc^-$. Therefore, for the remaining experiments, $KMeSO_4$ was used as the major salt in the pipette solution. In this chapter, it has been shown that SCs express medium and slow $Ca^{2+}$-dependent currents. Next, we directly tested if these $Ca^{2+}$-dependent currents are mediated by $K^+$ channels. In addition, the second hypothesis

(section 1.4.6 hypothesis 2) was addressed by testing if apamin-sensitive SK channels contribute to these currents.

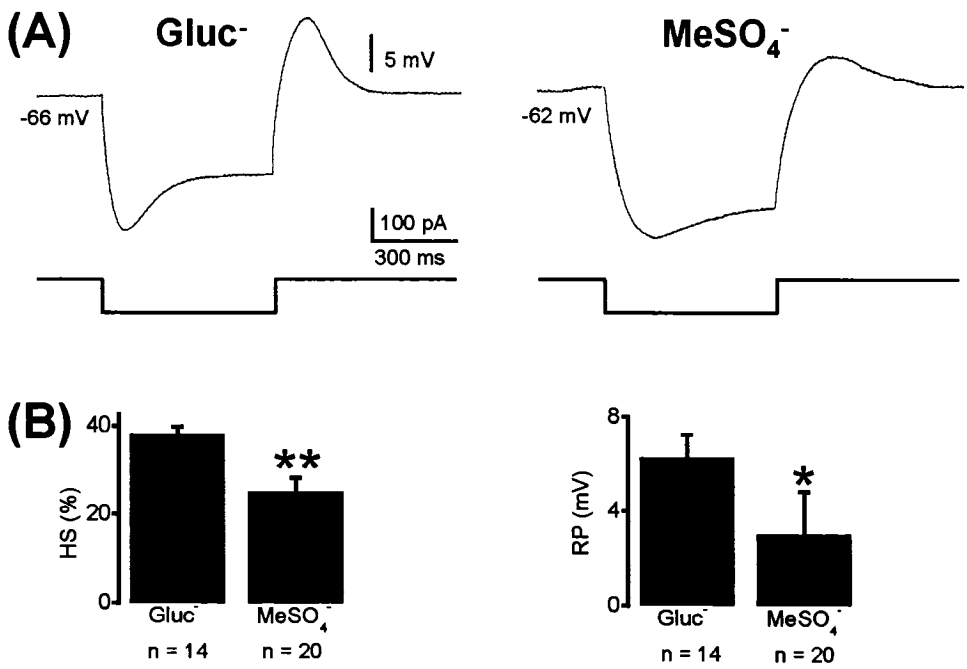


**Figure 3.1 Effect of intracellular $Gluc^-$ and $MeSO_4^-$ on h-current dependent sag in MEC layer II SCs.** *A*, Voltage responses of representative SCs patched with electrodes containing $Gluc^-$ (left) or $MeSO_4^-$ (right) showing the h-current dependent sag evoked by a 100 pA hyperpolarizing current pulse lasting 600 ms. *B*, Bar graphs comparing mean (± S.E.M.) HS% and RP evoked in SCs patched with $Gluc^-$ or $MeSO_4^-$. * denotes $p < 0.05$; ** denotes $p < 0.01$.

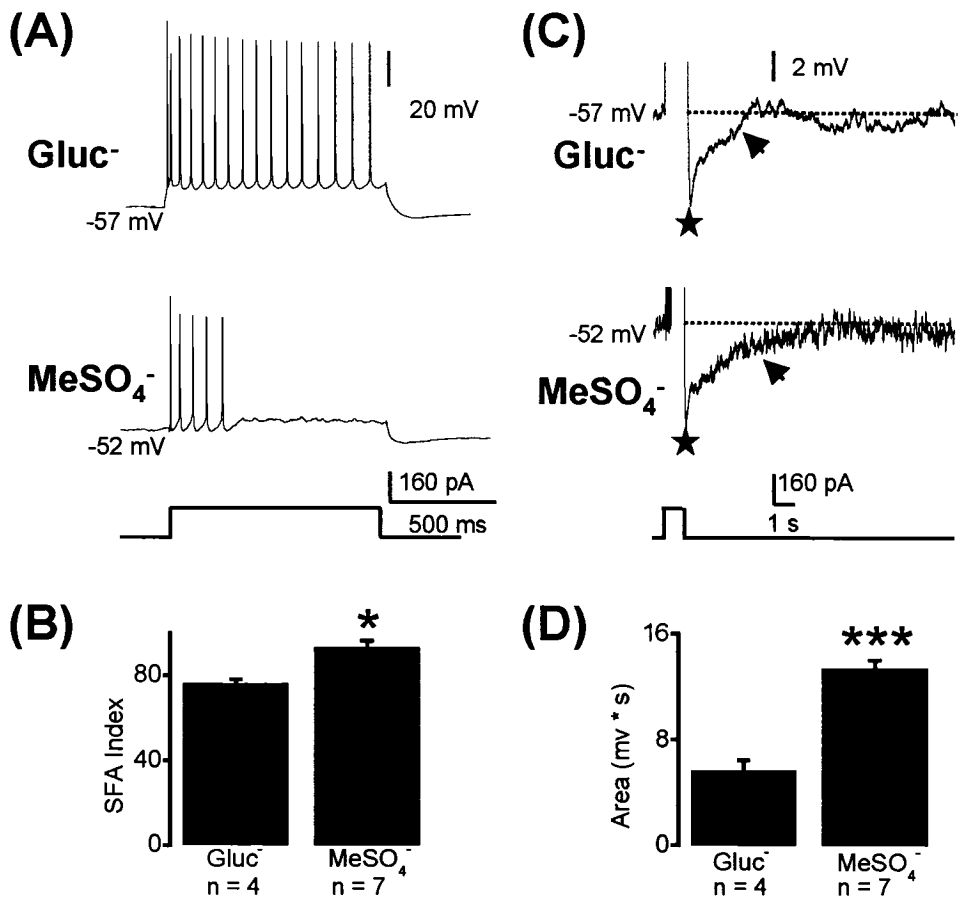


**Figure 3.2 Differential effect of intracellular $Gluc^-$ and $MeSO_4^-$ on SFA and the post-burst AHP in MEC layer II SCs.** The medium and slow post-burst AHPs are indicated by a star and arrow, respectively. *A*, Voltage responses of representative SCs patched with pipettes containing $Gluc^-$ (top) or $MeSO_4^-$ (bottom) showing differential SFA evoked by a 160 pA depolarizing current pulse lasting 1 sec. *B*, Bar graph showing the effect of pipette solution on the mean (± S.E.M.) SFA index observed in the two groups. *C*, Voltage responses of SCs patched with pipettes containing $Gluc^-$ (top) or $MeSO_4^-$ (bottom) showing differential post-burst AHP (same stimulating protocol as in *A*). *D*, Bar graph showing the effect of pipette solution on the mean (± S.E.M.) post- burst AHP area for both groups. * denotes $p < 0.05$; *** denotes $p < 0.001$.

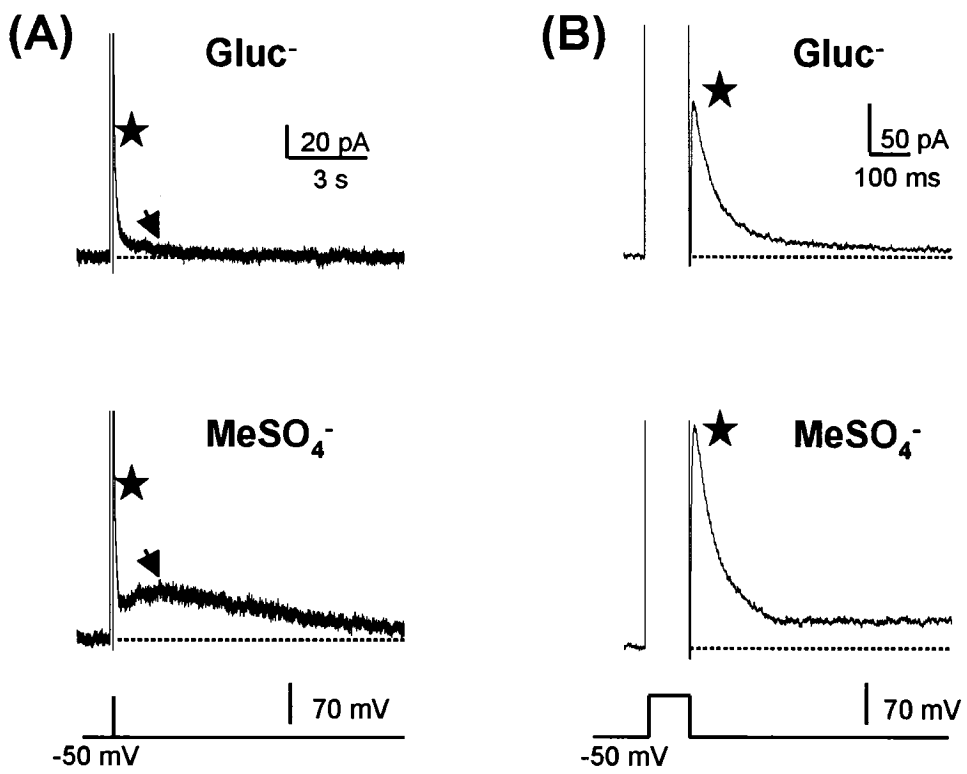


**Figure 3.3 $mI_{K(Ca)}$ and $sI_{AHP}$ in MEC layer II SCs.** *A*, Current responses of representative SCs patched with electrodes containing $Gluc^-$ (top) or $MeSO_4^-$ (bottom) showing $sI_{AHP}$ (denoted by arrow) evoked by a step depolarization to +20 mV lasting 100 ms from a holding potential of -50 mV (shown below the traces). *B*, Expanded view of the current traces in *A* in which $mI_{K(Ca)}$ (denoted by star) is clearly shown.

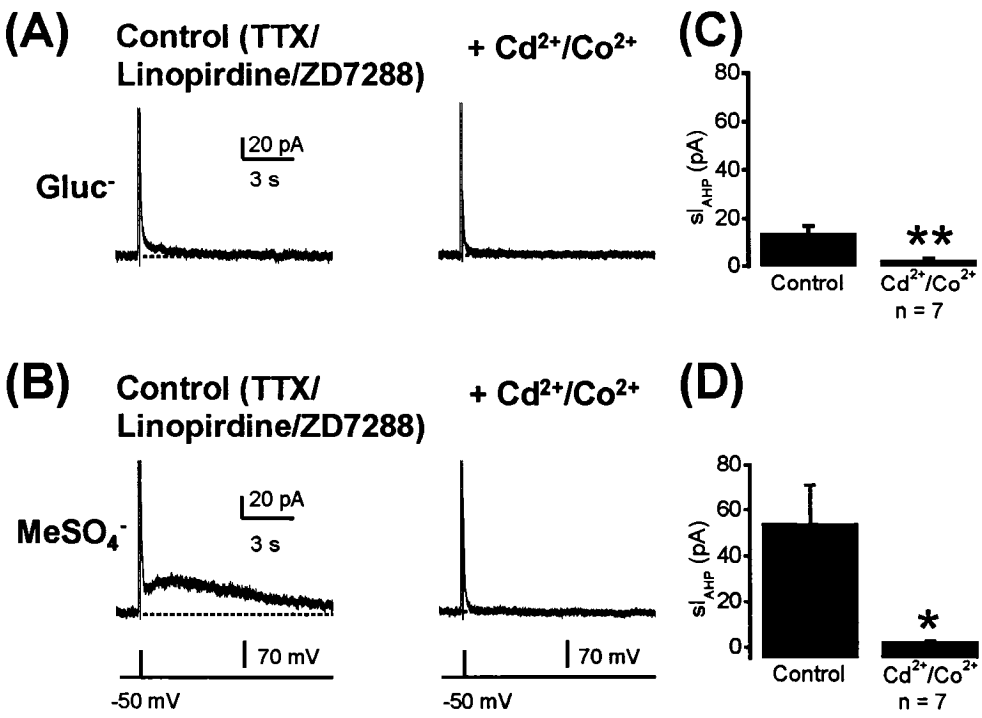


**Figure 3.4 $Ca^{2+}$-dependence of $sI_{AHP}$ in MEC layer II SCs.** *A,B* Current responses of representative SCs patched with electrodes containing $Gluc^-$ (*A*) or $MeSO_4^-$ (*B*) showing $sI_{AHP}$ before (left) and after (right) application of 300 μM $Cd^{2+}$ and 2 mM $Co^{2+}$. Currents were evoked by a step depolarization to +20 mV lasting 100 ms from a holding potential of -50 mV. *C, D* Bar graphs showing a significant decrease in mean (± S.E.M.) $sI_{AHP}$ amplitude after $Cd^{2+}/Co^{2+}$ application in the presence of intracellular $Gluc^-$ (*C*) or $MeSO_4^-$ (*D*). * denotes $p < 0.05$; ** denotes $p < 0.01$.

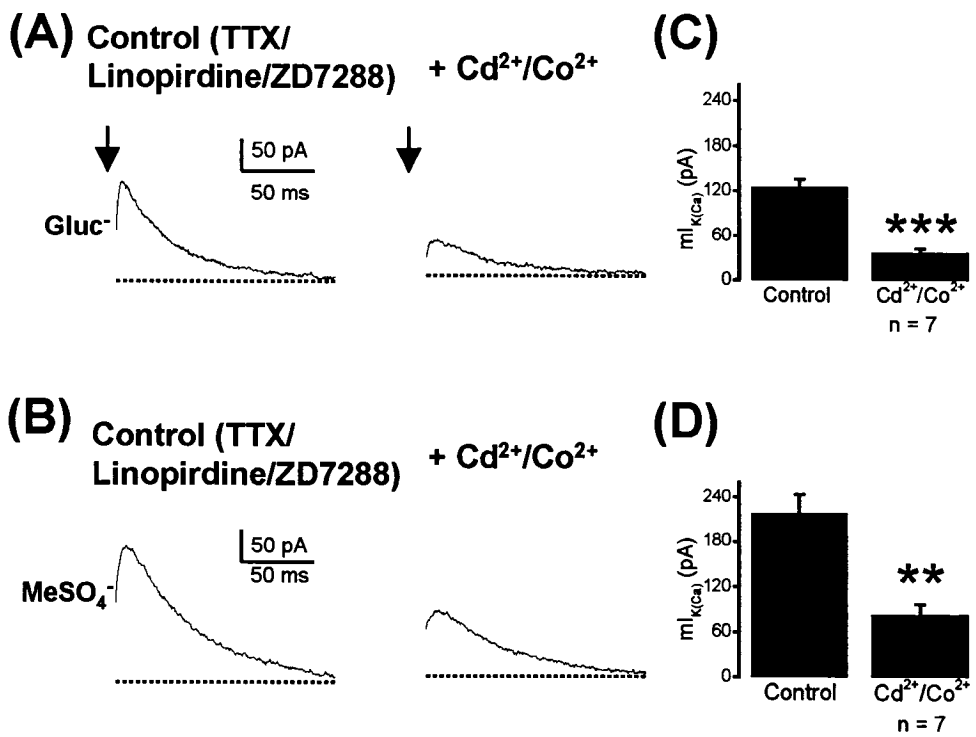


**Figure 3.5 $Ca^{2+}$-dependence of $mI_{K(Ca)}$ in MEC layer II SCs.** *A,B* Current responses of SCs patched with electrodes containing $Gluc^-$ (*A*) or $MeSO_4^-$ (*B*) showing $mI_{K(Ca)}$ before (left) and after (right) application of 300 μM $Cd^{2+}$ and 2 mM $Co^{2+}$. Currents were evoked by a step depolarization to +20 mV lasting 100 ms from a holding potential of -50 mV. Downward arrows represent the end of the depolarizing voltage step. *C, D* Bar graphs showing a significant decrease in mean (± S.E.M.) $mI_{K(Ca)}$ amplitude after $Cd^{2+}/Co^{2+}$ application in the presence of intracellular $Gluc^-$ (*C*) or $MeSO_4^-$ (*D*). ** denotes $p < 0.01$; *** denotes $p < 0.001$.

# CHAPTER 4: Apamin-insensitive $mI_{K(Ca)}$ and $sI_{AHP}$ are mediated by $K^+$ channels

## 4.1) Properties of $mI_{K(Ca)}$ and $sI_{AHP}$ in cortical neurons

It was revealed in chapter 3 that MEC layer II SCs contain medium and slow $Ca^{2+}$-dependent currents ($mI_{K(Ca)}$ and $sI_{AHP}$ - section 3.6). As explained in the introduction (see section 1.3.3 – 1.3.4 for explanation), it is important to determine the underlying ionic mechanisms of $mI_{AHP}$ and $sI_{AHP}$ in MEC layer II SCs. It was also mentioned that both the $Ca^{2+}$-dependent $mI_{AHP}$ and $sI_{AHP}$ are mediated by $K^+$ channels in most cortical neurons (section 1.4.2). However, it has not been tested if the $Ca^{2+}$-dependent $mI_{AHP}$ and $sI_{AHP}$ are mediated by $K^+$ channels in MEC layer II SCs (section 1.4.6 hypothesis 1). The $Ca^{2+}$-dependent $K^+$ component of $mI_{AHP}$ is mediated by apamin-sensitive SK channels in most cortical neurons (section 1.4.4). SK channels are small conductance $Ca^{2+}$-dependent $K^+$ ($K_{Ca}$) channels that are activated by $Ca^{2+}$ influx through voltage-gated calcium channels (section 1.4.4). It is not known whether these channels contribute to $mI_{AHP}$ in MEC layer II SCs (section 1.4.6 hypothesis 2) as well. To address these hypotheses (section 1.4.6 hypotheses 1 and 2), experiments were conducted to determine if $mI_{K(Ca)}$ and $sI_{AHP}$ are mediated by $K^+$ channels in MEC layer II SCs and if apamin-sensitive SK channels contribute to $mI_{AHP}$ in these cells.

## 4.2) Reversal potential of $mI_{K(Ca)}$ and $sI_{AHP}$

Experiments have been conducted on various types of neurons and have established that $mI_{K(Ca)}$ and $sI_{AHP}$ are mediated by $K^+$ channels (Alger and Nicoll, 1980; Connors et al., 1982; Constanti and Sim, 1987; Storm, 1989). Therefore, we examined in

MEC layer II SCs if the reversal potentials of $sI_{AHP}$ and $mI_{K(Ca)}$ were near the Nernst potential for $K^+$ under our conditions (-103 mV). From a holding potential of -50 mV, leak currents were evoked by applying a step hyperpolarization lasting 16 s to potentials ranging from -60 to -115 (Figure 6A inset) in the presence of 1 μM TTX, 20 μM linopirdine and 30 μM ZD-7288. Next, from a holding potential of -50 mV, $mI_{K(Ca)}$ and $sI_{AHP}$ were evoked in SCs by applying a 500 ms step depolarization to +20 mV followed by a step to test voltages ranging from -50 mV to -115 mV. The leak currents were subtracted from the depolarizing pulse-evoked currents to extract $sI_{AHP}$ and $mI_{K(Ca)}$. The top trace of Figure 4.1A shows $sI_{AHP}$ for a representative SC after subtraction of leak currents and the baseline current is marked by a solid red line. The $sI_{AHP}$ amplitude in SCs was measured (relative to baseline) at the time when the current was at its peak, after the full decay of $mI_{K(Ca)}$ (see section 2.5 for details). In SCs, the amplitude of $sI_{AHP}$ became smaller at more negative test voltages and reversed polarity between -90 mV and -100 mV (mean $sI_{AHP}$ amplitude = -94 ± 0.4 mV; n = 3; e.g. Figure 4.1A), close to the Nernst potential for $K^+$ (arrow $E_K$; Figure 4.1C left). The reversal potentials of other ions, such as $Na^+$ ($E_{Na}$ = ~ +75 mV) and $Cl^-$ ($E_{Cl}$ = ~ -46 mV) were much more positive than $E_K$ under our conditions. Therefore, it was concluded that $sI_{AHP}$ is mediated by $K^+$ channels in MEC layer II SCs. $mI_{K(Ca)}$ amplitude also decreased at more negative test voltages and reversed polarity between -80 mV and -90 mV (mean $mI_{K(Ca)}$ amplitude = -85 ± 1.7 mV; n = 3; e.g. Figure 4.1B), near $E_K$ (Figure 4.1C right) and far from the reversal potentials of other ions. This suggested that $mI_{K(Ca)}$ is also mediated by $K^+$ channels in MEC layer II SCs. Next, to address the second hypothesis (section 1.4.6 hypothesis 2), it was tested if apamin-sensitive SK channels (section 1.4.4) contribute to $mI_{AHP}$ and $sI_{AHP}$ in MEC layer II SCs.

## 4.3) Apamin-sensitive SK channels do not mediate $mI_{AHP}$ in MEC layer II SCs

To determine if SK channels contribute to $mI_{AHP}$ in MEC layer II SCs, $mI_{AHP}$ was evoked by applying a 100 ms depolarizing voltage step to +20 mV from a holding potential of -50 mV in the presence of 1 μM TTX before and after addition of apamin. Amplitudes and time constants of $mI_{AHP}$ were obtained through exponential fittings (see section 2.7 for details) of this current before and after 300 nM apamin application. $mI_{AHP}$ has been shown to be apamin-sensitive in most cortical cells (section 1.4.4); however, $mI_{AHP}$ decreased minimally in MEC layer II SCs after apamin application (230 ± 38 pA to 227 ± 37 pA; n = 9; p = 0.96; e.g. Figure 4.2A). The time constants of $mI_{AHP}$ did not change significantly after apamin application (48 ± 5.1 ms to 52 ± 6.6 ms; n = 9; p = 0.09). To examine if apamin has an effect on $mI_{AHP}$ in other EC neurons, we applied 300 nM apamin on MEC layer II non-stellate cells. Apamin significantly reduced $mI_{AHP}$ in MEC layer II non-SCs (166 ± 34 pA to 37 ± 5 pA; n = 3; $p < 0.05$; e.g. Figure 4.3A). These results indicated that apamin-sensitive SK channels do not contribute to $mI_{AHP}$ in MEC layer II SCs.

## 4.4) Apamin-sensitive SK channels do not mediate $sI_{AHP}$ in MEC layer II SCs

Next, it was tested if $sI_{AHP}$ (section 1.4.5) is apamin-sensitive in MEC layer II SCs. $sI_{AHP}$ did not change significantly after apamin application in SCs (16 ± 6 pA to 15 ± 6 pA; n = 9; p = 0.86; e.g. Figure 4.4A). Also, the time constants of $sI_{AHP}$ decay did not change significantly after apamin application (3.1 ± 0.4 s to 3.2 ± 0.6 s; n = 9; p = 0.88).

These results suggested that $sI_{AHP}$ is also apamin-insensitive in MEC layer II SCs. The apamin-insensitivity of $sI_{AHP}$ in MEC layer II SCs is consistent with what has been reported for other cortical cells (section 1.4.5).

## 4.5) Discussion

### *4.5.1) $mI_{K(Ca)}$ and $sI_{AHP}$ are mediated by $K^+$ channels*

Our experiments revealed that the mean reversal potentials of $mI_{K(Ca)}$ and $sI_{AHP}$ in MEC layer II SCs were very close to $E_K$ and far away from the Nernst potential of other ions (section 4.2). It is therefore concluded that both $mI_{K(Ca)}$ and $sI_{AHP}$ are mediated by $K^+$ channels in MEC layer II SCs, as found in other neurons (see section 1.4.2). However, the reversal potentials of $mI_{K(Ca)}$ and $sI_{AHP}$ in SCs were not exactly equivalent to $E_K$ (~ -103 mV) This may be due to several reasons: First, no correction was made for the errors caused by junction potentials, which may be up to ~ 4 mV under these conditions. In addition, $E_K$ was calculated based on ion concentrations and not ion activities, which would overestimate the magnitude of $E_K$ and thereby contribute to the discrepancy. $mI_{K(Ca)}$ amplitude was measured 20 ms after the peak of the current response in order to reduce the confounding effects of the inward capacitive transients present in the current traces when we stepped from the conditioning voltage (+20 mV) to test voltages below the holding potential (-50 mV) (see inset in Figure 4.1A for protocol used). However, only a component of this inward capacitive artifact was removed by subtracting leak currents evoked at each of the test voltages from the holding potential (-50 mV). Finally, it is possible that an additional current, which may not be mediated by $K^+$ channels, contributes to $mI_{AHP}$ in MEC layer II SCs and this current may be partly

responsible for the discrepancy observed. Although a discrepancy exists between $E_K$ and the reversal potential of $mI_{K(Ca)}$, the reversal potential of $mI_{K(Ca)}$ was close to $E_K$, indicating that $mI_{K(Ca)}$ is mediated predominantly by $K^+$ channels, as in other neurons.

### *4.5.2) Channels mediating $mI_{AHP}$ in MEC layer II SCs remain unknown*

The second hypothesis (section 1.4.6 hypothesis 2) was rejected as it was revealed that apamin-sensitive SK channels do not contribute to $mI_{AHP}$ in SCs (section 4.3). In addition, the positive control experiment showed that apamin application reduces $mI_{AHP}$ amplitude in MEC layer II non-SCs (section 4.3). This indicated that apamin-sensitive SK channels contribute to $mI_{AHP}$ in non-SCs. The EC has been shown to express mRNA coding for apamin-sensitive $K_{Ca}$ 2.2 and $K_{Ca}$ 2.3 subunits, as well as apamin-insensitive $K_{Ca}$ 2.1 subunits (Stocker and Pedarzani, 2000; D'Hoedt et al., 2004). The studies on MEC layer II non-SCs suggest that $mI_{AHP}$ may be mediated by $K_{Ca}$ 2.2 and/or $K_{Ca}$ 2.3 channels in these cells. On the other hand, the studies on MEC layer II SCs suggest that neither $K_{Ca}$ 2.2 nor $K_{Ca}$ 2.3 channels contribute to $mI_{AHP}$ in SCs. However, since $K_{Ca}$ 2.1 expression is also prominent in the EC (Stocker and Pedarzani, 2000; D'Hoedt et al., 2004), we initially thought that apamin-insensitive $K_{Ca}$ 2.1 channels may contribute to $mI_{AHP}$ in MEC layer II SCs. However, studies have suggested that $K_{Ca}$ 2.1 subunits cannot form functional channels by themselves (D'Hoedt et al., 2004), indicating that homomeric channels consisting of $K_{Ca}$ 2.1 subunits are not likely to contribute to $mI_{AHP}$ in MEC layer II SCs. The $K_{Ca}$ currents $I_C$ and $I_{AHP}$ make up $mI_{K(Ca)}$ (see section 1.4.3 for review) in hippocampal neurons, where $I_{AHP}$ is mediated by apamin-sensitive SK channels and $I_C$ is mediated by BK channels (section 1.4.3). BK channels are big conductance voltage- and $Ca^{2+}$-dependent $K^+$ channels known to contribute to $mI_{AHP}$ in

hippocampal neurons (Storm, 1990; Sah and McLachlan, 1991). It has been shown that $I_C$ may be blocked by applying 1 mM TEA in cortical neurons (Sah, 1996). To test whether $I_C$ is a component of $mI_{K(Ca)}$ in MEC layer II SCs, 1 mM TEA was applied in SCs. This experiment revealed that $mI_{K(Ca)}$ is reduced by ~14% in SCs (n = 2) after application of TEA. This suggested that only a small component of $mI_{K(Ca)}$ is mediated by TEA-sensitive BK channels. Therefore, it can be concluded that the remaining current is neither mediated by SK nor BK channels. In addition, since the voltage-dependent currents were blocked in SCs by applying linopirdine and ZD-7288 (section 4.3), the remaining medium duration current is neither $I_M$ nor $I_h$. Thus, the molecular nature of the channels mediating $mI_{AHP}$ in MEC layer II SCs remains unknown.

### *4.5.3) Apamin-sensitive SK channels do not mediate $sI_{AHP}$ in MEC layer II SCs*

Our experiments revealed that $sI_{AHP}$ is apamin-insensitive in MEC layer II SCs; and therefore, is not mediated by SK channels (section 4.4). This finding is consistent with other reports that have shown the apamin-insensitivity of $sI_{AHP}$ in various cortical neurons (section 1.2.5). As mentioned in the introduction (section 1.2.5) that there are currently no known pharmacological blockers of $sI_{AHP}$. However, it has been demonstrated that $sI_{AHP}$ may be inhibited via modulation through the cAMP pathway (section 1.2.6). Therefore, to test the final hypothesis (section 1.3 hypothesis 3), it was investigated whether $sI_{AHP}$ and SFA are inhibited in MEC layer II SCs via modulation by the cAMP pathway.

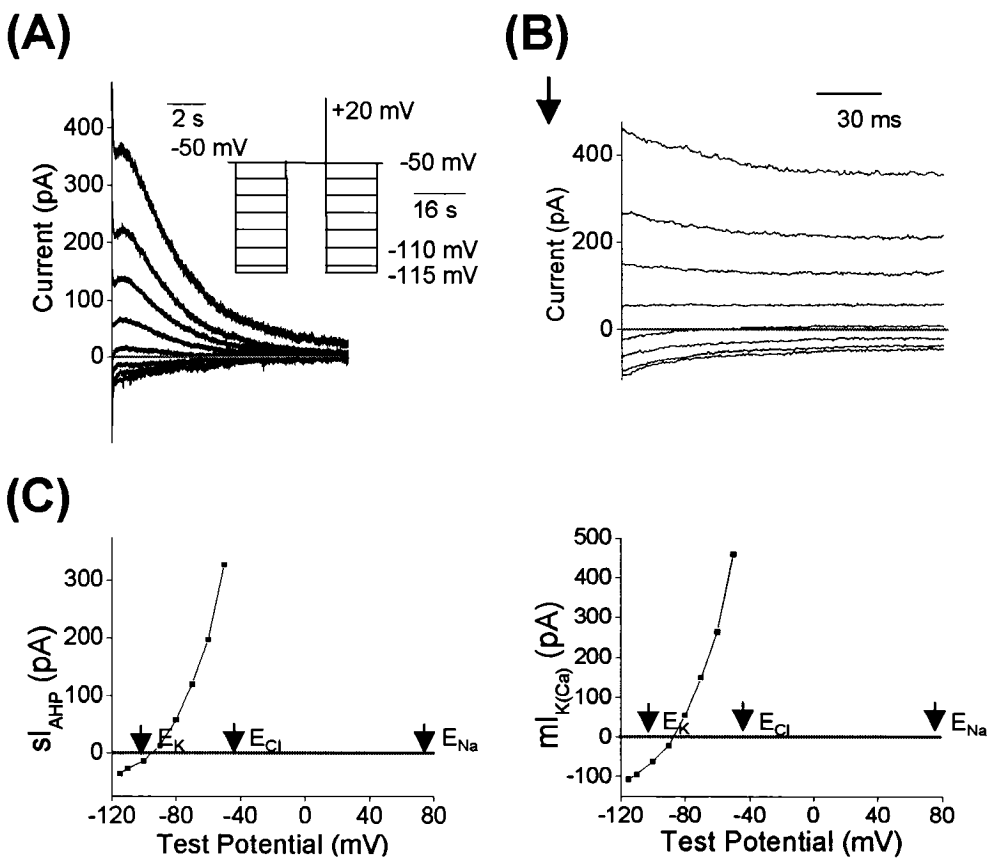


**Figure 4.1 $mI_{K(Ca)}$ and $sI_{AHP}$ are mediated by $K^+$ channels in MEC layer II SCs.** *A,B* Current responses of a representative SC showing the reversal potentials of $sI_{AHP}$ (*A*) and $mI_{K(Ca)}$ (*B*) obtained by subtracting leak currents (evoked by applying a step hyperpolarization lasting 16 s to potentials ranging from -60 to -115; see inset) from depolarizing pulse-evoked currents (evoked in by applying a 500 ms long step depolarization to +20 mV followed by a step to test voltages ranging from -50 mV to -115 mV; see inset). Baseline current is indicated with a red solid line. *C,* Plots showing the resulting $sI_{AHP}$ (left) and $mI_{K(Ca)}$ (right) amplitudes for a representative SC. Arrows denote $E_K$ (~ -103 mV), $E_{Na}$ (~ +75 mV) and $E_{Cl}$ (~ -46 mV).

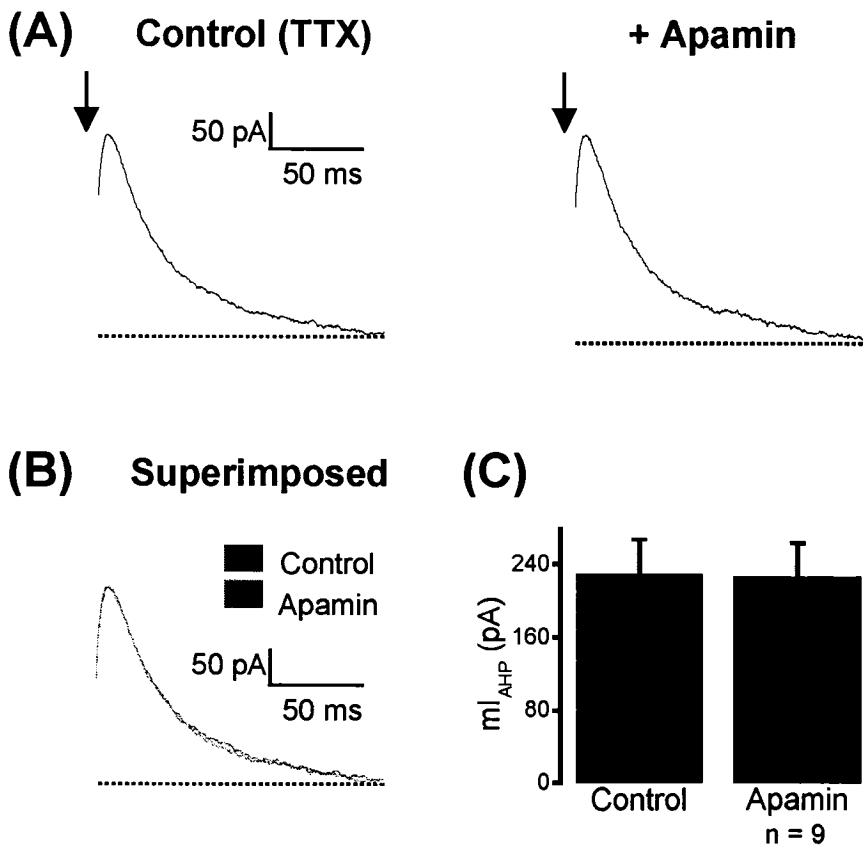


**Figure 4.2 Apamin-sensitive SK channels do not mediate $mI_{AHP}$ in MEC layer II SCs.** *A*, Current responses of a representative SC showing $mI_{AHP}$ (evoked by a step depolarization to +20 mV lasting 100 ms from a holding potential of -50 mV) before (left) and after (right) application of 300 nM apamin. Downward arrows represent the end of the depolarizing voltage step. *B*, Superimposed traces from *A* showing $mI_{AHP}$ before (blue) and after (red) apamin application. *C*, Bar graph showing no significant difference in mean (± S.E.M.) $mI_{AHP}$ amplitude between control and apamin treated cells.

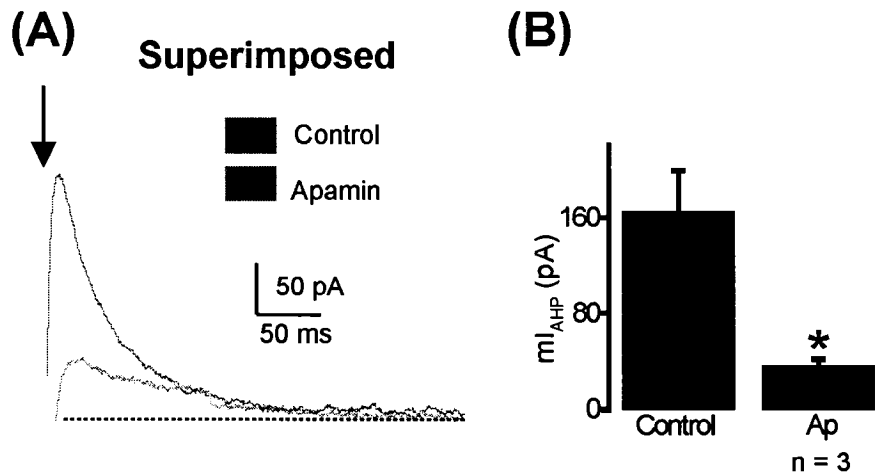


**Figure 4.3 Apamin-sensitive SK channels contribute to $mI_{AHP}$ in MEC layer II non-SCs.** *A*, Superimposed current responses of a representative non-SC showing $mI_{AHP}$ (evoked by a step depolarization to +20 mV lasting 100 ms from a holding potential of -50 mV) before (blue) and after (red) application of 300 nM apamin (Ap). The downward arrow represents the end of the depolarizing voltage step. *B*, Bar graph showing a significant decrease in mean (± S.E.M.) $mI_{AHP}$ amplitude after apamin application. * denotes $p < 0.05$.

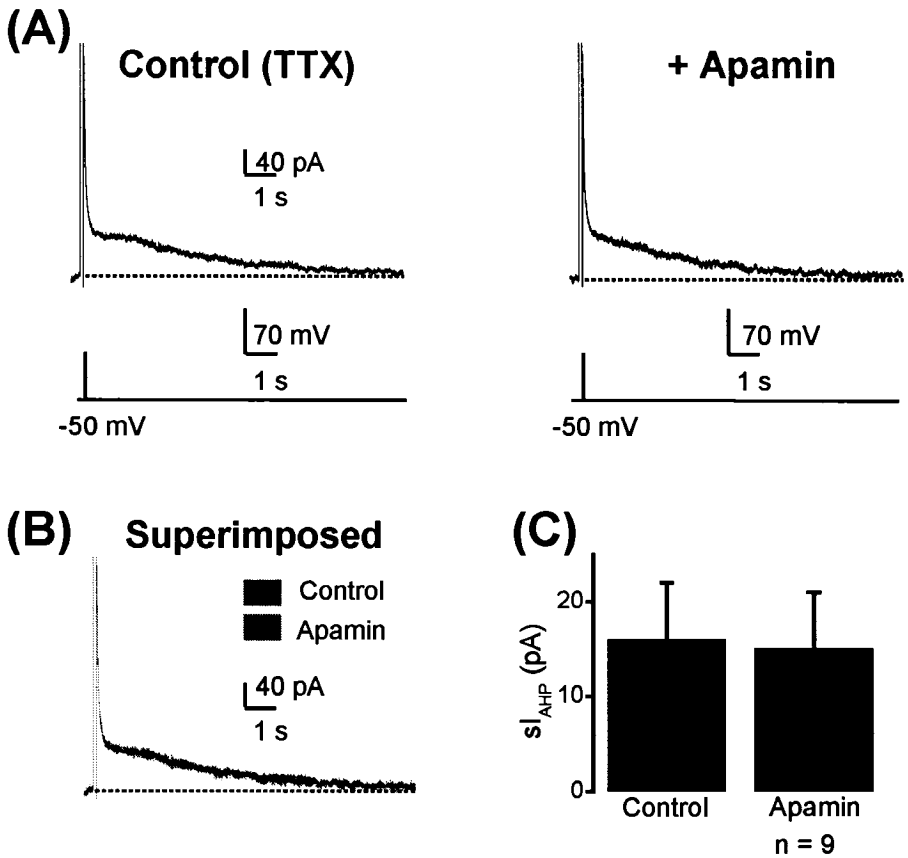


**Figure 4.4 Apamin-sensitive SK channels do not mediate $sI_{AHP}$ in MEC layer II SCs.** *A*, Current responses of a representative SC showing $sI_{AHP}$ (evoked by a step depolarization to +20 mV lasting 100 ms from a holding potential of –50 mV) before (left) and after (right) application of 300 nM apamin. *B*, Superimposed traces from *A* showing $sI_{AHP}$ before (blue) and after (red) apamin application. *C*, Bar graph showing no significant difference in mean (± S.E.M.) $sI_{AHP}$ amplitude between control (blue) and apamin (red) treated cells.

# CHAPTER 5: Modulation of $mI_{K(Ca)}$, $sI_{AHP}$ and SFA in MEC layer II SCs

## 5.1) Modulation of $sI_{AHP}$ and SFA in cortical neurons

Previous work has shown that activation of the cAMP pathway can attenuate $sI_{AHP}$ without affecting $mI_{K(Ca)}$ in cortical neurons (section 1.4.6). SFA is also reduced after activation of the cAMP pathway in cortical neurons (section 1.4.6). The effects of cAMP on $sI_{AHP}$ and SFA are mediated by PKA in hippocampal neurons (section 1.4.6). However, it is not known if $sI_{AHP}$ and SFA are reduced by activation of the cAMP pathway in MEC layer II SCs. Thus, according to the third hypothesis (see section 1.4.6 hypothesis 3), it was tested if inhibitory modulation by the cAMP pathway can reduce $sI_{AHP}$ and SFA in SCs.

## 5.2) Inhibitory modulation of $mI_{K(Ca)}$ and $sI_{AHP}$ through activation of the cAMP pathway

It has been shown in hippocampal cells that $sI_{AHP}$ is suppressed after activation of the cAMP pathway, an effect known to be mediated by PKA (section 1.4.6). Application of forskolin is known to activate adenylate cyclase, an enzyme that synthesizes cAMP (Nicoll, 1988; Nicoll et al., 1990). Also, Ro 20-1724 inhibits the phosphodiesterase that converts cAMP back into adenosine mono-phosphate (AMP) (Kandel, 2000). It was hypothesized that application of forskolin and Ro 20-1724 to activate the cAMP pathway in MEC layer II SCs would suppress $sI_{AHP}$, while not affecting $mI_{K(Ca)}$ (section 1.4.6) To evoke $mI_{K(Ca)}$ and $sI_{AHP}$, a 100 ms long depolarizing voltage step to +20 mV was applied from a holding potential of -50 mV in the presence of 1 μM TTX, 20 μM linopirdine and

30 μM ZD-7288. Amplitudes and time constants of $mI_{K(Ca)}$ and $sI_{AHP}$ were obtained through exponential fittings (see section 2.7 for details) of this current before and after application of 50 uM forskolin and 200 uM Ro 20-1724. $sI_{AHP}$ amplitude decreased significantly (by 66 ± 8 %) after application of forskolin and Ro 20-1724 in SCs (30 ± 6 pA to 8 ± 1 pA; n = 8; p = 0.008; e.g. Figure 5.1A). Reduction of $sI_{AHP}$ was expected and consistent with results from previous studies of cortical cells (section 1.4.6). Surprisingly, $mI_{K(Ca)}$ amplitude also decreased significantly ( by 61 ± 14 %) in SCs after forskolin and Ro 20-1724 application (189 ± 24 pA to 60 ± 14 pA; n = 8; p = 0.003; e.g. Figure 5.1B). These results suggested that both $mI_{K(Ca)}$ and $sI_{AHP}$ are inhibited via modulation through the cAMP pathway.

## 5.3) Inhibitory modulation of SFA through activation of the cAMP pathway

Since $mI_{K(Ca)}$ and $sI_{AHP}$ are known to contribute to SFA in various cortical neurons (section 1.4.2), we wanted to determine if reduction of these currents can also affect SFA in SCs. We evoked spike-trains by applying a 150 pA current pulse lasting 6 seconds. The mean RMP was near -62 mV and was adjusted by DC current injection (mean membrane potential was -60 ± 1 mV in these experiments). An adaptation index (see section 2.6 for calculation of SFA index) was used to quantify SFA in MEC layer II SCs. The adaptation index decreased after application of 25 μM forskolin (87 ± 4 to 77 ± 5; n = 4; p = 0.006; e.g. Figure 5.2A) in SCs. From this experiment, it was concluded that SFA is also inhibited via modulation through the cAMP pathway in MEC layer II SCs.

## 5.4) Discussion

### *5.4.1) Inhibitory modulation of $sI_{AHP}$ and SFA by activation of PKA*

The results presented here indicate that $sI_{AHP}$ and SFA are both inhibited via modulation through the cAMP pathway in MEC layer II SCs (section 5.2-5.3). In hippocampal cells, the effects of cAMP on $sI_{AHP}$ and SFA are mediated by PKA (section 1.4.6). In particular, SFA and $sI_{AHP}$ may be suppressed in hippocampal neurons by the PKA-dependent phosphorylation of the $sI_{AHP}$ channel itself or some other intermediary protein or by the activation of other enzymatic pathways (section 1.4.6). Similarly, it is possible that PKA-dependent phosphorylation is involved in regulating the inhibitory modulation of $sI_{AHP}$ channels in MEC layer II SCs.

### *5.4.2) Inhibitory modulation of $mI_{K(Ca)}$ by PKA activation*

A surprising observation was that $mI_{K(Ca)}$ was also reduced after applying forskolin and Ro 20-1724 (section 5.2). This component has not been reported to be subject to modulation in other cortical neurons (section 1.4.6). Yet, as mentioned above (see section 5.3), ~ 61% of $mI_{K(Ca)}$ was suppressed upon exposure to forskolin and Ro 20-1724. We hypothesize that the channel underlying the forskolin and Ro 20-1724-sensitive $mI_{K(Ca)}$ component in SCs is inhibited by PKA-dependent modulation.

### *5.4.3) $mI_{K(Ca)}$ and $sI_{AHP}$ may underlie SFA in MEC layer II SCs*

Our studies suggest that both $mI_{K(Ca)}$ and $sI_{AHP}$ may undergo inhibitory modulation by activation of the cAMP-PKA pathway in MEC layer II SCs (section 5.2). In addition, it is possible that PKA-activation reduces SFA in these cells (section 5.3). In

these experiments, the SFA index (see section 2.6 for calculation of SFA index) was calculated using the first and last instantaneous firing frequencies (i.e. before and after forskolin application). In particular, the mean time in SCs of the occurrence of the second action potential in the spike-burst was ~ 19 ms under control conditions. As a result, it is probable that there was only minimal activation of $mI_{K(Ca)}$ and $sI_{AHP}$ at the time of the second action potential. Moreover, it is likely that both $mI_{K(Ca)}$ and $sI_{AHP}$ were fully activated at the time of the occurrence of the last two action potentials in the spike-burst under control conditions. In addition, both of these currents may be inhibited by activation of PKA (see section 5.4.1 – 5.4.2). Thus, it is likely that both $mI_{K(Ca)}$ and $sI_{AHP}$ are inhibited during the spike-burst after application of forskolin; and therefore, both of these currents may underlie SFA in MEC layer II SCs. However, our experiments did not reveal the specific contributions of $mI_{K(Ca)}$ and $sI_{AHP}$ to SFA in MEC layer II SCs. It has been shown that $mI_{K(Ca)}$ and $sI_{AHP}$ contribute to the early and late phases of SFA, respectively, in cortical neurons (section 1.4.2). By conducting additional experiments to clarify the contribution of each of these currents to SFA in SCs, we can determine if these currents contribute to the early and late phases of SFA in these neurons as well.

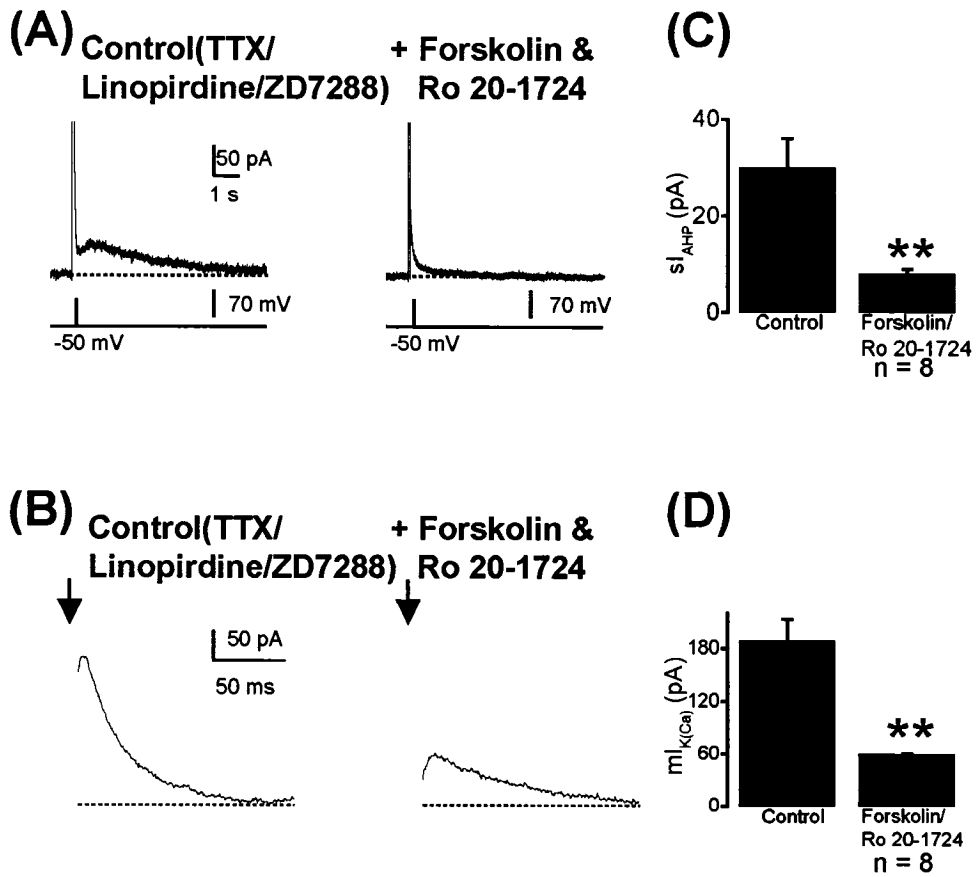


**Figure 5.1 Inhibitory modulation of $mI_{K(Ca)}$ and $sI_{AHP}$ through activation of The cAMP pathway.** *A,B* Current responses of a representative SC showing $sI_{AHP}$ (*A*) and $mI_{K(Ca)}$ (*B*) (evoked by a step depolarization to +20 mV lasting 100 ms from a holding potential of -50 mV) before (left) and after (right) application of 50 μM forskolin and 200 μM Ro20-1724. Downward arrows represent the end of the depolarizing voltage step. *C,D* Bar graphs showing mean (± S.E.M.) $sI_{AHP}$ (*C*) and mean (± S.E.M.) $mI_{K(Ca)}$ (*D*) amplitude before and after forskolin/Ro20-1724 application. ** denotes $p < 0.01$.

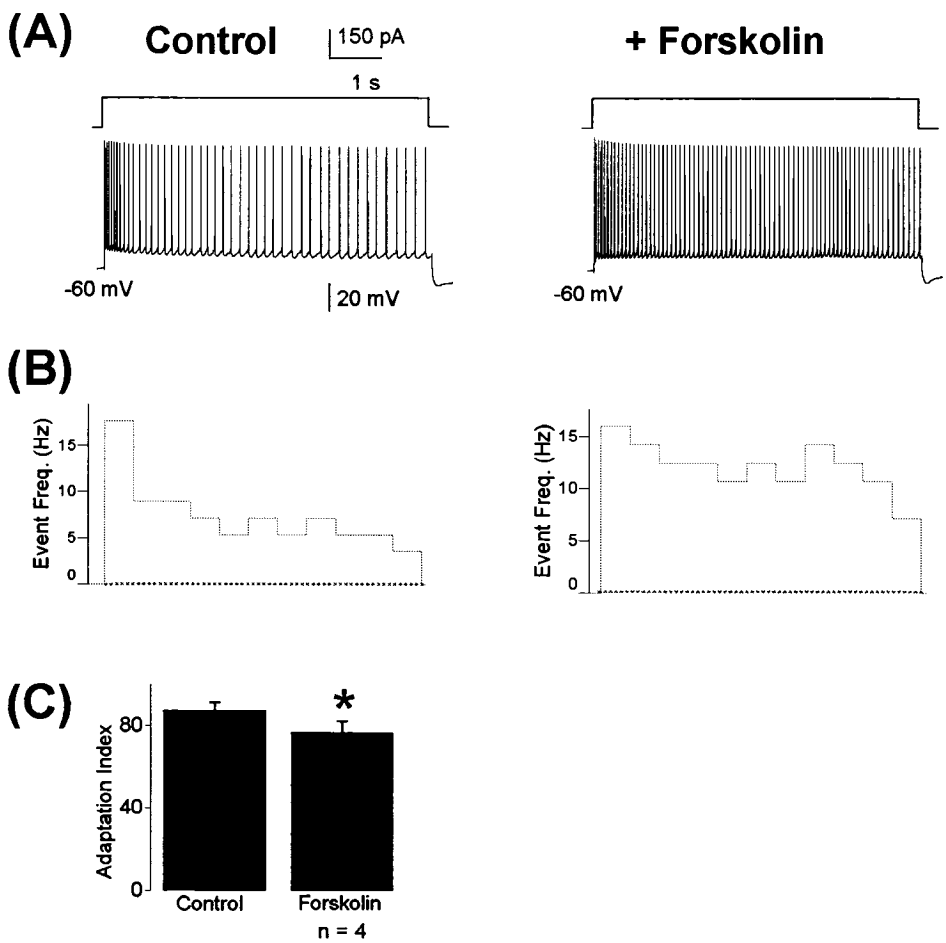


**Figure 5.2 Inhibitory modulation of SFA through activation of the cAMP pathway.** *A*, Voltage responses of a representative SC showing a spike-burst (evoked by a 150 pA depolarizing current pulse lasting 6 sec) before (left) and after (right) application of 25 μM forskolin. *B*, Corresponding frequency graph (bin width = 565 ms) of the SC shown in *A* in which the red dotted line marks a frequency of 0 Hz. *C*, Bar graph showing a significant decrease in the mean (± S.E.M.) SFA index after forskolin application. ** denotes $p < 0.01$.

# CHAPTER 6: General Discussion

## 6.1) Summary of rationale for studies

Investigators have used various tasks (i.e. DMS or DMNS; see section 1.2.5 for description) to study WM function in animals (section 1.2.6). Although the functional role of the EC during these WM tasks is mostly unknown, neurons from superficial layers of the EC can be briefly excited by presentation of a stimulus, and they have been found to exhibit a non-adapting increase in firing activity during the delay period of these tasks (section 1.2.6). Likewise, brief excitatory stimuli delivered to these cells by current pulses applied during whole-cell patch clamp recording from EC slices have been shown to evoke post-burst non-adapting after-discharges in MEC layer II SCs treated with carbachol (see Figure 1.3B top). Thus, this post-burst activity observed at the single-cell level may be a neuronal correlate of the post-stimulus activity displayed during the delay period in WM tasks (section 1.3.3 – 1.3.4). An important feature of sustained activity observed *in-vivo* and *in-vitro* in SCs is that it is non-adapting, even for periods lasting tens of seconds (see Figure 1.3B bottom). Moreover, although SFA is observed in SCs under control conditions *in-vitro*, SFA is reduced in the presence of carbachol (section 1.3.4). In addition, previous studies, which employed intracellular sharp electrode recording techniques, have shown that MEC layer II SCs exhibit SFA as well as medium and slow AHPs (section 1.4.1 – 1.4.2). Therefore, it was proposed that inhibitory modulation of the currents that underlie SFA may permit the non-adapting nature of post-burst after-discharges in these cells (section 1.3.4). The currents underlying SFA in MEC layer II SCs were not known at the time. The aim of this thesis was therefore to

determine the ionic mechanisms and possible modulators of these currents in SCs by performing experiments to test the specific hypotheses outlined at the end of section 1.4.6.

## 6.2) Summary of results

The present study of MEC layer II SCs tested each of the formulated hypotheses (see section 1.4.6 hypotheses 1 – 3) and revealed several novel findings. First, it showed for the first time that MEC layer II SCs express medium ($mI_{K(Ca)}$) and slow ($sI_{AHP}$) AHP currents (section 3.5), which are both mediated by $Ca^{2+}$-dependent $K^+$ channels (section 3.6, 4.2). Furthermore, our studies demonstrated that $mI_{AHP}$ is not mediated by apamin-sensitive SK channels (section 4.3) in MEC layer II SCs, whereas $mI_{AHP}$ is sensitive to apamin in non-SCs (section 4.3). Finally, the present studies showed that $mI_{K(Ca)}$, $sI_{AHP}$ and SFA undergo inhibitory modulation in SCs by activation of the cAMP-PKA pathway (section 5.2, 5.3). To our knowledge, this is the first demonstration of a cortical cell in which $mI_{K(Ca)}$ may be subject to inhibitory modulation by PKA activation.

## 6.3) Functional implications

### *6.3.1) Activation of PKA during WM*

WM is thought to be active on a scale of seconds or minutes (Goldman-Rakic, 1995) and various WM tasks have been employed in animal and human subjects to study the neural mechanisms underlying WM (Baddeley and Warrington, 1970; Cave and Squire, 1992; Suzuki et al., 1997; Young et al., 1997). We proposed that a reduction of the currents underlying SFA in SCs may permit the non-adapting nature of post-burst

after-discharges (section 1.3.4). Our experiments suggested that SFA is reduced in MEC layer II SCs via PKA activation (section 5.2). PKA activation may be important for SCs to exhibit post-burst after-discharges, a possible neuronal correlate of post-stimulus delay firing observed in the superficial EC during WM tasks.

In our studies, the cAMP-PKA pathway was presumably activated by adenylate cyclase, a forskolin-activated enzyme that synthesizes cAMP (section 5.2). Although forskolin is used to activate PKA *in-vitro*, it is not endogenous in the brain. *In-vivo,* PKA is activated through a signaling process which requires the binding of various monoaminergic neurotransmitters to G-protein coupled receptors (see section 1.4.6). For example, noradrenaline, serotonin and histamine, released from the axon-terminals of brainstem neurons, bind to specific types of G-protein coupled receptors in the cortex to activate adenylate cyclase, leading to the activation of the cAMP-PKA pathway (Pedarzani and Storm, 1993). Monoaminergic projections are known to innervate most cortical neurons, including EC neurons (Pedarzani and Storm, 1993). Furthermore, it has been proposed that monoaminergic modulation of the cortex may control its functional state, thereby leading to shifts from sleep to wakefulness, attention, modulation of sensory perception, arousal, emotions and cognitive functions (Chu and Bloom, 1973; Steriade and Llinas, 1988; McCormick, 1989; Steriade and McCarley, 1990). It has also been hypothesized that inhibitory modulation of $sI_{AHP}$ may be an important mechanism for the effects of these neurotransmitters on the functional state of the cortex (Pedarzani and Storm, 1993). Although some of these behavioral states (i.e. attention, arousal) are activated during WM processing (Nielson and Jensen, 1994; Awh and Jonides, 2001; Woodson et al., 2003), such a correlation has not been identified in the EC specifically. Moreover, the modulatory effects of monoaminergic transmitters on MEC layer II SCs

have not been measured during WM tasks. As a result, it is currently difficult to provide direct evidence to support the idea that monoaminergic modulation *in vivo* may enable delay firing observed in neurons from the superficial EC in general, and MEC layer II SCs in particular. Future work will be required to determine if monoaminergic modulation *in-vivo* can enable post-stimulus delay firing activity in EC neurons.

As described in the introduction (section 1.2.3), lesion and imaging studies have shown that the MTL is important for WM function (Baddeley and Warrington, 1970; Cave and Squire, 1992; Stern et al., 2001). In particular, imaging studies revealed the involvement of the MTL in WM for novel stimuli (Stern et al., 2001). Thus, although monoaminergic modulation is believed to influence the functional state of the entire cortex, modulation of the MTL may be responsible for maintaining WM for novel stimuli. In addition, due to the central location of the EC in the MTL, and of MEC layer II SCs in particular (see Figure 1.2), monoaminergic modulation of G-protein coupled receptors located in SCs may play an important role in maintaining WM. Future work is required to establish whether monoaminergic modulation of EC neurons plays an important role during WM tasks.

### *6.3.2) Parallel information processing in layer II of the MEC*

Previous studies have shown that SCs and non-SC cells from layer II of the MEC exhibit different electrophysiological characteristics (Alonso and Klink, 1993; Klink and Alonso, 1997a, b). From the present studies with MEC layer II neurons, a pharmacological difference was also revealed between SCs and non-SCs. Specifically, it was determined that apamin-sensitive SK channels contribute to $mI_{AHP}$ in MEC layer II non-SCs, but not in SCs (section 4.3). These results suggest that either apamin-sensitive

SK channels may not be expressed in SCs, or if these channels are present there, they do not contribute to $mI_{AHP}$. These findings also indicate that different channels may underlie $mI_{AHP}$ in the two types of EC layer II neurons. In particular, apamin-sensitive channels encoded by $K_{Ca}$ 2.2 and/or $K_{Ca}$ 2.3 may contribute to $mI_{K(Ca)}$ in non-SCs, whereas the $Ca^{2+}$-dependent $K^+$ channel that contributes to $mI_{K(Ca)}$ in SCs is still unknown. Future experiments are required to identify the channel underlying $mI_{K(Ca)}$ in SCs. In particular, it may be possible that $K_{Ca}$ 2.1 subunits (see section 1.4.4) form functional channels *in-vivo* and contribute to $mI_{K(Ca)}$ in MEC layer II SCs. One way to test the contribution of $K_{Ca}$ 2.1 channels toward $mI_{K(Ca)}$ in SCs is by genetic suppression of SK1 expression in these cells.

Modulation through the cAMP-PKA pathway significantly reduces $mI_{K(Ca)}$ in MEC layer II SCs (see section 5.2 – 5.3). However, numerous studies have suggested that the apamin-sensitive $mI_{AHP}$ is not subject to inhibitory modulation by the cAMP-PKA pathway in cortical cells (Stocker, 2004; Stocker et al., 2004). Therefore, we predict that, unlike $mI_{AHP}$ of SCs, the apamin-sensitive $mI_{AHP}$ in MEC layer II non-SCs is not subject to inhibitory modulation by the cAMP-PKA pathway. If this hypothesis is correct, a modulatory difference may also exist between the two subtypes of principle principal neurons in layer II of the MEC. Since both types of cells project to the hippocampus (see section 1.2.4), we propose that two parallel channels of information, with differential physiological, pharmacological and modulatory properties can operate in this projection. Further experiments are required to define the function of these separate pathways to MEC-hippocampal region information processing and WM.

# References


Ahmed B, Anderson JC, Douglas RJ, Martin KA, Whitteridge D (1998) Estimates of the net excitatory currents evoked by visual stimulation of identified neurons in cat visual cortex. Cereb Cortex 8:462-476.

Alger BE, Nicoll RA (1980) Epileptiform burst afterhyperolarization: calcium-dependent potassium potential in hippocampal CA1 pyramidal cells. Science 210:1122-1124.

Alonso A, Llinas RR (1989) Subthreshold Na+-dependent theta-like rhythmicity in stellate cells of entorhinal cortex layer II. Nature 342:175-177.

Alonso A, Klink R (1993) Differential electroresponsiveness of stellate and pyramidal-like cells of medial entorhinal cortex layer II. J Neurophysiol 70:128-143.

Awh E, Jonides J (2001) Overlapping mechanisms of attention and spatial working memory. Trends Cogn Sci 5:119-126.

Baddeley A (2003) Working memory: looking back and looking forward. Nat Rev Neurosci 4:829-839.

Baddeley AD, Warrington EK (1970) Amnesia and the distinction between long- and short-term memory. Journal of Verbal Learning and Behavior 9:176 - 189.

Barkai E, Hasselmo ME (1994) Modulation of the input/output function of rat piriform cortex pyramidal cells. J Neurophysiol 72:644-658.

Benda J, Longtin A, Maler L (2005) Spike-frequency adaptation separates transient communication signals from background oscillations. J Neurosci 25:2312-2321.

BoSmith RE, Briggs I, Sturgess NC (1993) Inhibitory actions of ZENECA ZD7288 on whole-cell hyperpolarization activated inward current (If) in guinea-pig dissociated sinoatrial node cells. Br J Pharmacol 110:343-349.

Burwell RD, Amaral DG (1998a) Perirhinal and postrhinal cortices of the rat: interconnectivity and connections with the entorhinal cortex. J Comp Neurol 391:293-321.

Burwell RD, Amaral DG (1998b) Cortical afferents of the perirhinal, postrhinal, and entorhinal cortices of the rat. J Comp Neurol 398:179-205.

Burwell RD, Witter MP, Amaral DG (1995) Perirhinal and postrhinal cortices of the rat: a review of the neuroanatomical literature and comparison with findings from the monkey brain. Hippocampus 5:390-408.

Cave CB, Squire LR (1992) Intact verbal and nonverbal short-term memory following damage to the human hippocampus. Hippocampus 2:151-163.

Chu N, Bloom FE (1973) Norepinephrine-containing neurons: changes in spontaneous discharge patterns during sleeping and waking. Science 179:908-910.

Connors BW, Gutnick MJ, Prince DA (1982) Electrophysiological properties of neocortical neurons in vitro. J Neurophysiol 48:1302-1320.

Constanti A, Sim JA (1987) Calcium-dependent potassium conductance in guinea-pig olfactory cortex neurones in vitro. J Physiol 387:173-194.

Corkin S, Amaral DG, Gonzalez RG, Johnson KA, Hyman BT (1997) H. M.'s medial temporal lobe lesion: findings from magnetic resonance imaging. J Neurosci 17:3964-3979.

D'Hoedt D, Hirzel K, Pedarzani P, Stocker M (2004) Domain analysis of the calcium-activated potassium channel SK1 from rat brain. Functional expression and toxin sensitivity. J Biol Chem 279:12088-12092.

Dickson CT, Magistretti J, Shalinsky MH, Fransen E, Hasselmo ME, Alonso A (2000) Properties and role of I(h) in the pacing of subthreshold oscillations in entorhinal cortex layer II neurons. J Neurophysiol 83:2562-2579.

Fransen E (2005) Functional role of entorhinal cortex in working memory processing. Neural Netw 18:1141-1149.

Goldman-Rakic PS (1995) Cellular basis of working memory. Neuron 14:477-485.

Haas HL, Greene RW (1986) Effects of histamine on hippocampal pyramidal cells of the rat in vitro. Exp Brain Res 62:123-130.

Hille B (2001) Ion Channels of Excitable Membranes. Sunderland: Sinauer Associates, Inc.

Insausti R, Amaral DG, Cowan WM (1987a) The entorhinal cortex of the monkey: III. Subcortical afferents. J Comp Neurol 264:396-408.

Insausti R, Amaral DG, Cowan WM (1987b) The entorhinal cortex of the monkey: II. Cortical afferents. J Comp Neurol 264:356-395.

Insausti R, Herrero MT, Witter MP (1997) Entorhinal cortex of the rat: cytoarchitectonic subdivisions and the origin and distribution of cortical efferents. Hippocampus 7:146-183.

Kandel ER, Schwartz, J. H., Jessell, T. M. (2000) Principles of Neural Science, 4th Edition. New York: McGraw-Hill.

Kao CY (1972) Pharmacology of tetrodotoxin and saxitoxin. Fed Proc 31:1117-1123.

Klink R, Alonso A (1993) Ionic mechanisms for the subthreshold oscillations and differential electroresponsiveness of medial entorhinal cortex layer II neurons. J Neurophysiol 70:144-157.

Klink R, Alonso A (1997a) Muscarinic modulation of the oscillatory and repetitive firing properties of entorhinal cortex layer II neurons. J Neurophysiol 77:1813-1828.

Klink R, Alonso A (1997b) Morphological characteristics of layer II projection neurons in the rat medial entorhinal cortex. Hippocampus 7:571-583.

Lancaster B, Nicoll RA (1987) Properties of two calcium-activated hyperpolarizations in rat hippocampal neurones. J Physiol 389:187-203.

Leonard BW, Amaral DG, Squire LR, Zola-Morgan S (1995) Transient memory impairment in monkeys with bilateral lesions of the entorhinal cortex. J Neurosci 15:5637-5659.

Lorenzon NM, Foehring RC (1992) Relationship between repetitive firing and afterhyperpolarizations in human neocortical neurons. J Neurophysiol 67:350-363.

Madison DV, Nicoll RA (1982) Noradrenaline blocks accommodation of pyramidal cell discharge in the hippocampus. Nature 299:636-638.

Madison DV, Nicoll RA (1984) Control of the repetitive discharge of rat CA 1 pyramidal neurones in vitro. J Physiol 354:319-331.

Madison DV, Nicoll RA (1986) Cyclic adenosine 3',5'-monophosphate mediates beta-receptor actions of noradrenaline in rat hippocampal pyramidal cells. J Physiol 372:245-259.

Magistretti J, Ma L, Shalinsky MH, Lin W, Klink R, Alonso A (2004) Spike patterning by Ca2+-dependent regulation of a muscarinic cation current in entorhinal cortex layer II neurons. J Neurophysiol 92:1644-1657.

McCormick DA (1989) Cholinergic and noradrenergic modulation of thalamocortical processing. Trends Neurosci 12:215-221.

Meunier M, Bachevalier J, Mishkin M, Murray EA (1993) Effects on visual recognition of combined and separate ablations of the entorhinal and perirhinal cortex in rhesus monkeys. J Neurosci 13:5418-5432.

Nicoll RA (1988) The coupling of neurotransmitter receptors to ion channels in the brain. Science 241:545-551.

Nicoll RA, Malenka RC, Kauer JA (1990) Functional comparison of neurotransmitter receptor subtypes in mammalian central nervous system. Physiol Rev 70:513-565.

Nielson KA, Jensen RA (1994) Beta-adrenergic receptor antagonist antihypertensive medications impair arousal-induced modulation of working memory in elderly humans. Behav Neural Biol 62:190-200.

Olson IR, Moore KS, Stark M, Chatterjee A (2006a) Visual working memory is impaired when the medial temporal lobe is damaged. J Cogn Neurosci 18:1087-1097.

Olson IR, Page K, Moore KS, Chatterjee A, Verfaellie M (2006b) Working memory for conjunctions relies on the medial temporal lobe. J Neurosci 26:4596-4601.

Pasternak T, Greenlee MW (2005) Working memory in primate sensory systems. Nat Rev Neurosci 6:97-107.

Pedarzani P, Storm JF (1993) PKA mediates the effects of monoamine transmitters on the K+ current underlying the slow spike frequency adaptation in hippocampal neurons. Neuron 11:1023-1035.

Pennefather P, Lancaster B, Adams PR, Nicoll RA (1985) Two distinct Ca-dependent K currents in bullfrog sympathetic ganglion cells. Proc Natl Acad Sci U S A 82:3040-3044.

Sah P (1996) Ca(2+)-activated K+ currents in neurones: types, physiological roles and modulation. Trends Neurosci 19:150-154.

Sah P, McLachlan EM (1991) Ca(2+)-activated K+ currents underlying the afterhyperpolarization in guinea pig vagal neurons: a role for Ca(2+)-activated Ca2+ release. Neuron 7:257-264.

Sah P, Isaacson JS (1995) Channels underlying the slow afterhyperpolarization in hippocampal pyramidal neurons: neurotransmitters modulate the open probability. Neuron 15:435-441.

Schmolck H, Stefanacci L, Squire LR (2000) Detection and explanation of sentence ambiguity are unaffected by hippocampal lesions but are impaired by larger temporal lobe lesions. Hippocampus 10:759-770.

Schmolck H, Kensinger EA, Corkin S, Squire LR (2002) Semantic knowledge in patient H.M. and other patients with bilateral medial and lateral temporal lobe lesions. Hippocampus 12:520-533.

Schnee ME, Brown BS (1998) Selectivity of linopirdine (DuP 996), a neurotransmitter release enhancer, in blocking voltage-dependent and calcium-activated potassium currents in hippocampal neurons. J Pharmacol Exp Ther 286:709-717.

Schwindt PC, Spain WJ, Foehring RC, Chubb MC, Crill WE (1988a) Slow conductances in neurons from cat sensorimotor cortex in vitro and their role in slow excitability changes. J Neurophysiol 59:450-467.

Schwindt PC, Spain WJ, Foehring RC, Stafstrom CE, Chubb MC, Crill WE (1988b) Multiple potassium conductances and their functions in neurons from cat sensorimotor cortex in vitro. J Neurophysiol 59:424-449.

Scoville WB, Milner B (1957) Loss of recent memory after bilateral hippocampal lesions. J Neurol Neurosurg Psychiatry 20:11-21.

Shah MM, Mistry M, Marsh SJ, Brown DA, Delmas P (2002) Molecular correlates of the M-current in cultured rat hippocampal neurons. J Physiol 544:29-37.

Squire LR, Stark CE, Clark RE (2004) The medial temporal lobe. Annu Rev Neurosci 27:279-306.

Steriade M, Llinas RR (1988) The functional states of the thalamus and the associated neuronal interplay. Physiol Rev 68:649-742.

Steriade M, McCarley, eds (1990) Brainstem control of wakefulness and sleep. New York: Plenum Publishing Corp.

Stern CE, Sherman SJ, Kirchhoff BA, Hasselmo ME (2001) Medial temporal and prefrontal contributions to working memory tasks with novel and familiar stimuli. Hippocampus 11:337-346.

Stocker M (2004) Ca(2+)-activated K+ channels: molecular determinants and function of the SK family. Nat Rev Neurosci 5:758-770.

Stocker M, Pedarzani P (2000) Differential distribution of three Ca(2+)-activated K(+) channel subunits, SK1, SK2, and SK3, in the adult rat central nervous system. Mol Cell Neurosci 15:476-493.

Stocker M, Krause M, Pedarzani P (1999) An apamin-sensitive Ca2+-activated K+ current in hippocampal pyramidal neurons. Proc Natl Acad Sci U S A 96:4662-4667.

Stocker M, Hirzel K, D'Hoedt D, Pedarzani P (2004) Matching molecules to function: neuronal Ca2+-activated K+ channels and afterhyperpolarizations. Toxicon 43:933-949.

Storm JF (1989) An after-hyperpolarization of medium duration in rat hippocampal pyramidal cells. J Physiol 409:171-190.

Storm JF (1990) Potassium currents in hippocampal pyramidal cells. Prog Brain Res 83:161-187.

Suzuki WA, Amaral DG (1994) Perirhinal and parahippocampal cortices of the macaque monkey: cortical afferents. J Comp Neurol 350:497-533.

Suzuki WA, Miller EK, Desimone R (1997) Object and place memory in the macaque entorhinal cortex. J Neurophysiol 78:1062-1081.

Tomita H, Ohbayashi M, Nakahara K, Hasegawa I, Miyashita Y (1999) Top-down signal from prefrontal cortex in executive control of memory retrieval. Nature 401:699-703.

Velumian AA, Zhang L, Pennefather P, Carlen PL (1997) Reversible inhibition of IK, IAHP, Ih and ICa currents by internally applied gluconate in rat hippocampal pyramidal neurones. Pflugers Arch 433:343-350.

Villalobos C, Shakkottai VG, Chandy KG, Michelhaugh SK, Andrade R (2004) SKCa channels mediate the medium but not the slow calcium-activated afterhyperpolarization in cortical neurons. J Neurosci 24:3537-3542.

Vogalis F, Harvey JR, Furness JB (2002) TEA- and apamin-resistant K(Ca) channels in guinea-pig myenteric neurons: slow AHP channels. J Physiol 538:421-433.

Vogalis F, Storm JF, Lancaster B (2003) SK channels and the varieties of slow after-hyperpolarizations in neurons. Eur J Neurosci 18:3155-3166.

Wang XJ (2001) Synaptic reverberation underlying mnemonic persistent activity. Trends Neurosci 24:455-463.

Woodson JC, Macintosh D, Fleshner M, Diamond DM (2003) Emotion-induced amnesia in rats: working memory-specific impairment, corticosterone-memory correlation, and fear versus arousal effects on memory. Learn Mem 10:326-336.

Young BJ, Otto T, Fox GD, Eichenbaum H (1997) Memory representation within the parahippocampal region. J Neurosci 17:5183-5195.

Zhang L, Weiner JL, Valiante TA, Velumian AA, Watson PL, Jahromi SS, Schertzer S, Pennefather P, Carlen PL (1994) Whole-cell recording of the Ca(2+)-dependent slow afterhyperpolarization in hippocampal neurones: effects of internally applied anions. Pflugers Arch 426:247-253.

Zifa E, Fillion G (1992) 5-Hydroxytryptamine receptors. Pharmacol Rev 44:401-458.

# Appendix 1 - Permissions

This appendix contains the emails granting the rights and permissions of the authors and publishers of the various figures used in the introduction.

Although fonts and spacing have been formatted to conform with the style of the thesis, none of the text of the messages included in the e-mails cited below has been edited or modified.

## Appendix 1.1) Figure 1.1 permissions

**Figure 1.1 permission granted by Wiley-Liss, Inc. a subsidiary of John Wiley & Sons, Inc. for:**

**Figure 1A of Burwell RD, Amaral DG (1998a) Cortical afferents of the perirhinal, postrhinal, and entorhinal cortices of the rat. J Comp Neurol 398:179-205**

Dear Mr. Khawaja:

Please be advise that permission is granted to reuse material from Journal of Comparative Neurology 1998: 398, 179-205 in your forthcoming thesis which will be published by McGill University. Credit to our work much appear on every page where our material appears with the following acknowledgement "Reprinted with permission of Wiley-Liss, Inc. a subsidiary of John Wiley & Sons, Inc." Please Note: No rights are granted to use content that appears in the work with credit to another source.

Good luck with your thesis

Sincerely,

Sheik Safdar
Permissions Assistant
John Wiley & Sons, Inc.

**Figure 1.4 permission granted by Dr. Paola Pedarzani for:**

**Figure 3A of Stocker M, Krause M, Pedarzani P (1999) An apamin-sensitive Ca2+-activated K+ current in hippocampal pyramidal neurons. Proc Natl Acad Sci U S A 96:4662-4667.**

Dear Farhan,

It was our pleasure!
You have my permission to use the PNAS fig. 3A for your thesis.

All the best!
Paola

Hi Dr. Pedarzani,

First of all, thank you again for inviting me to present my work at the symposium.. I really enjoyed the meeting and the city as well.. Also, I wish you the very best in your future endeavors!

Can I please have your permission to use figure 3A from the PNAS paper ('99) for my thesis (see below).. Also, can you please forward me the contact info for Michael Krause.

Regards,

Farhan Khawaja